Global and Planetary Change 188 (2020) 103149

Contents lists available at ScienceDirect

Global and Planetary Change

journal homepage: www.elsevier.com/locate/gloplacha

Invited review article

Multidecadal modulations of key metrics of global climate change

Nathaniel C. Johnson[a,b,*], Dillon J. Amaya[c], Qinghua Ding[d,e], Yu Kosaka[f], Hiroki Tokinaga[g], Shang-Ping Xie[c]

[a] Atmospheric and Oceanic Sciences Program, Princeton University, Princeton, NJ 08540, USA
[b] National Oceanic and Atmospheric Administration/Geophysical Fluid Dynamics Laboratory, Princeton, NJ 08540, USA
[c] Scripps Institution of Oceanography, University of California, San Diego, La Jolla, CA 92093-0206, USA
[d] Department of Geography, University of California, Santa Barbara, CA 93106, USA
[e] Earth Research Institute, University of California, Santa Barbara, CA 93106, USA
[f] Research Center for Advanced Science and Technology, University of Tokyo, 4-6-1 Komaba, Meguro-ku, Tokyo 153-8904, Japan
[g] Research Institute for Applied Mechanics, Kyushu University, Kasuga, Fukuoka 816-8580, Japan

ARTICLE INFO

Keywords:
Global warming slowdown
Climate change metrics
Pacific decadal variability
Atlantic multidecadal variability
Polar amplification
Warm Arctic/cold continents
Hadley cell expansion

ABSTRACT

Widespread public and scientific interest in the recent global warming hiatus and related multidecadal climate variability stimulated a surge in our understanding of key metrics of global climate change. While seeking explanations for the nearly steady global mean temperature from late 1990s through the early 2010s, the scientific community also grappled with concomitant and seemingly inconsistent changes in other metrics. For example, over that period, Arctic sea ice experienced a rapid decline but Antarctic sea ice expanded slightly, summertime warm extremes continued to rise without evidence of a pause, and the expanding Hadley cell trend maintained its course. In this article, we review recent advances in understanding the multidecadal variability of these metrics of global climate change, focusing on how internal multidecadal variability may reconcile differences between projected and recently observed trends and apparent inconsistencies between recent trends in some metrics. We emphasize that the impacts of global scale, naturally occurring patterns on multidecadal timescales, most notably the Pacific and Atlantic Multidecadal Variability, tend to be more regionally heterogeneous than those of radiatively forced change, which weakens the relationship between local climate impacts and global mean temperature on multidecadal timescales. We conclude this review with a summary of current challenges and opportunities for progress.

1. Introduction

The climate system has experienced rapid warming since pre-industrial times, and many of the observed changes since the mid-20th century are unprecedented over decades to millennia (IPCC, 2014). The secular rise in global mean surface temperature (GMST) has been accompanied by changes of regional significance, including rising sea levels, changes in the likelihood and strength of extreme weather and climate events, a widening of the tropical belt, and rapid loss of land and sea ice. As a consequence of these changes and the consistency in simulations with state-of-the-art global climate models (GCMs), many of these metrics of global climate change have been detected in the observational record and attributed to increasing greenhouse gas (GHG) concentrations (Bindoff et al., 2013).

Despite the robustness of these observed climate changes on multidecadal to centennial timescales, apparent discrepancies between observed and expected changes in these metrics have challenged our understanding of global climate variability and change. The recent surface warming slowdown, often referred to as the global warming hiatus, is an example that received considerable public and scientific scrutiny. For a period from the late 1990s until the early 2010s, GMST remained nearly steady despite continued increasing GHG concentrations, sparking intense interest in determining the cause of the differences between observed and modelled surface temperature changes (Easterling and Wehner, 2009; Fyfe et al., 2016; Xie and Kosaka, 2017; Liu and Xie, 2018). This surge of scientific research significantly advanced understanding of the role of the tropical Pacific Ocean on global mean temperature (Meehl et al., 2011; Kosaka and Xie, 2013; Meehl et al., 2013; England et al., 2014; Amaya et al., 2015; Wu et al., 2019), called attention to data biases in our temperature record (Cowtan and

* Corresponding author at: NOAA/Geophysical Fluid Dynamics Laboratory, Princeton University Forrestal Campus, 201 Forrestal Rd., Princeton, NJ 08540-6649, USA.
E-mail address: Nathaniel.Johnson@noaa.gov (N.C. Johnson).

https://doi.org/10.1016/j.gloplacha.2020.103149
Received 31 October 2019; Received in revised form 14 February 2020; Accepted 27 February 2020
Available online 04 March 2020

Way, 2014; Karl et al., 2015) and radiative forcing (Schmidt et al., 2014), and opened dialogue about how such variations in GMST should be communicated (Lewandowsky et al., 2015; Fyfe et al., 2016). Although the concepts of internal climate variability and data uncertainties were already ingrained within the climate science community (even if inadequately communicated to the general public (Easterling and Wehner, 2009)), the global warming hiatus stimulated the climate science community to fill important gaps in our knowledge regarding the sources of deviation from the long-term trend for one of the most closely monitored metrics of global climate change—GMST.

The global warming hiatus further challenged our understanding of global climate variability and change through the consideration of other well-known metrics and their relationship with GMST. For example, despite GMST holding relatively steady, the occurrence of hot extremes over land continued to increase (Coumou and Rahmstorf, 2012; Kamae et al., 2014; Seneviratne et al., 2014; Johnson et al., 2018), Arctic sea ice continued its rapid decline (Vaughan et al., 2013), and Hadley cell expansion accelerated (Allen and Kovilakam, 2017; Amaya et al., 2018; Staten et al., 2018). These contrasting changes indicate that these metrics of global climate change may track GMST in counterintuitive ways. Such counterintuitive behavior can be reconciled by recent studies that have elucidated the differences between regional patterns associated with internal climate variability and radiatively forced changes associated with GHG warming.

In this review, we highlight recent advances in understanding the multidecadal modulations of several metrics of global climate change, focusing on the contrasting regional and temporally episodic patterns of change associated with modes of internal climate variability with the more spatially uniform and temporally monotonic changes associated with GHG warming. These recent studies have sharpened our understanding of the impacts of the dominant modes of internal climate variability on multidecadal timescales, particularly with respect to Pacific Decadal Variability (PDV) and Atlantic Multidecadal Variability (AMV). We focus on several iconic metrics of global climate change – GMST change, Arctic sea ice decline, Antarctic sea ice variability, global extreme temperature occurrence changes, and Hadley cell expansion – but the broader themes likely apply to other metrics as well. This rapid progress ensures that the climate science community is better prepared to address decadal-timescale deviations from the expected changes in these metrics, like the apparent GMST hiatus, but several challenges remain. This review concludes with a discussion of these challenges and pathways for progress.

2. Dominant modes of internal multidecadal variability

Given that many of the metrics of global climate change are strongly impacted by same internal modes of climate variability, we offer a brief summary of the dominant modes of PDV and AMV. (For more thorough reviews of these topics, see, for example, Henley et al. (2017) for PDV and Zhang et al. (2019c) for AMV.) A key difference between each of these modes and the pattern of sea surface warming induced by increasing greenhouse gases is the degree of spatial heterogeneity. To first order, the expected pattern of anthropogenically forced sea surface warming is spatially uniform except for the subpolar North Atlantic, although the spatial variations of sea surface temperature (SST) change (e.g., enhanced warming in the equatorial eastern Pacific) has important consequences for changes in the mean and variability of tropical rainfall (e.g., Xie et al., 2010; Power et al., 2013; Cai et al., 2014). In contrast, the leading internal modes of PDV and AMV are much more spatially heterogeneous, with high-amplitude SST anomalies (SSTA) of both signs (Fig. 1a,b). This difference in spatial heterogeneity in SST pattern is a key distinguishing feature between the response to GHG warming and internal modes of climate variability, and this difference has important consequences for the regional scale multidecadal variations discussed throughout this review.

2.1. Pacific decadal variability

The PDV, also referred to as the Interdecadal Pacific Oscillation (IPO; Power et al., 1999, Henley et al., 2015), is a pattern of variability that encompasses the Pacific Decadal Oscillation (PDO) in the North Pacific (Mantua et al., 1997), the South PDO (SPDO) in the South Pacific (Chen and Wallace, 2015), and the El Niño-Southern Oscillation-(ENSO)-like decadal variability in the tropical Pacific (Nitta and Yamada, 1989; Zhang et al., 1997). The PDV features an equatorially symmetric pattern of SST anomalies (Fig. 1a). The observed time series (Fig. 1e) features decadal to multidecadal periods of preferred phase but without a clearly identifiable single frequency (the reason that some prefer the "variability" terminology over "oscillation"). The positive phase dominated the period from the mid-1970s through late 1990s, and the subsequent period that encompassed the global warming hiatus featured a notable shift to negative phase dominance. Although the PDV is identified through the Pacific SST field, its influence extends well beyond the Pacific, impacting regional- and global-scale climate on multidecadal timescales, as discussed more thoroughly in the following sections.

The extratropical North PDO features an SST anomaly dipole with one lobe in the central North Pacific extending westward along the Kuroshio-Oyashio extension, and the other along the west coast of North America (Fig. 1a). Studies have identified that the PDO consists of multiple physical processes. In particular, the PDO can be decomposed into two components, one of which is forced remotely by the tropical Pacific variability and the other driven by atmospheric stochastic forcing (Newman et al., 2016). Both components are tied to variability of the Aleutian low associated with the Pacific-North American (PNA) pattern (Wallace and Gutzler, 1981), which is a preferred mode of variability anchored geographically through interactions with the zonally asymmetric background state and transient eddy activity. The two components therefore share a similar structure and are embedded in the basin-wide PDV pattern. A reddened ocean response to the atmospheric forcing and adjustments through ocean Rossby waves shape the PDO SST anomalies and timescale. They potentially feed back to the atmosphere, forming an air-sea coupled mode (Zhang and Delworth, 2015).

A coupled model study by Zhang et al., 2018b suggests that the South Pacific counterpart of the PDV is predominantly a response to forcing from the tropical Pacific through the Pacific-South American pattern (Karoly, 1989), the Southern Hemisphere (SH) atmospheric counterpart to the PNA. There is an internally driven component of the SPDO, but its structure is distinct from the tropical-forced component with a lack of SST anomalies along the South Pacific Convergence Zone (Zhang et al. (2018b)). When forced by the tropics, the PDO and SPDO covary and form the basin-wide PDV. Indeed, in the ensemble spread of the tropical Pacific pacemaker simulations where the tropical Pacific-forced variability is subtracted, the correlation between the PDO and SPDO vanishes (Zhang et al. (2018b)). The high inter-hemispheric symmetry also supports this hypothesis (Henley, 2017; Liu and Di Lorenzo, 2018).

Note, however, that this result does not preclude the possibility that the extratropical North and South Pacific anomalies drive or feed back to the tropical anomalies via atmospheric (Okumura, 2013; Amaya, 2019) and oceanic (Gu and Philander, 1997; Luo et al., 2003; Tatebe et al., 2013; Farneti et al., 2014) pathways. Additional potential drivers of the PDV include inter-basin influences from the Atlantic (McGregor et al., 2014; Li et al., 2015; Chikamoto et al., 2016; Kucharski et al., 2016) and Indian Ocean (Luo et al., 2012; Han et al., 2014; Mochizuki et al., 2016; Dong and McPhaden, 2017) through Walker circulation changes.

The PDV is primarily a mode of internal climate variability, but several studies have revealed possible influences of external forcing, including solar (Meehl et al., 2009), volcanic aerosol (Wang et al., 2012b; Maher et al., 2015), anthropogenic aerosol (Allen et al., 2014;

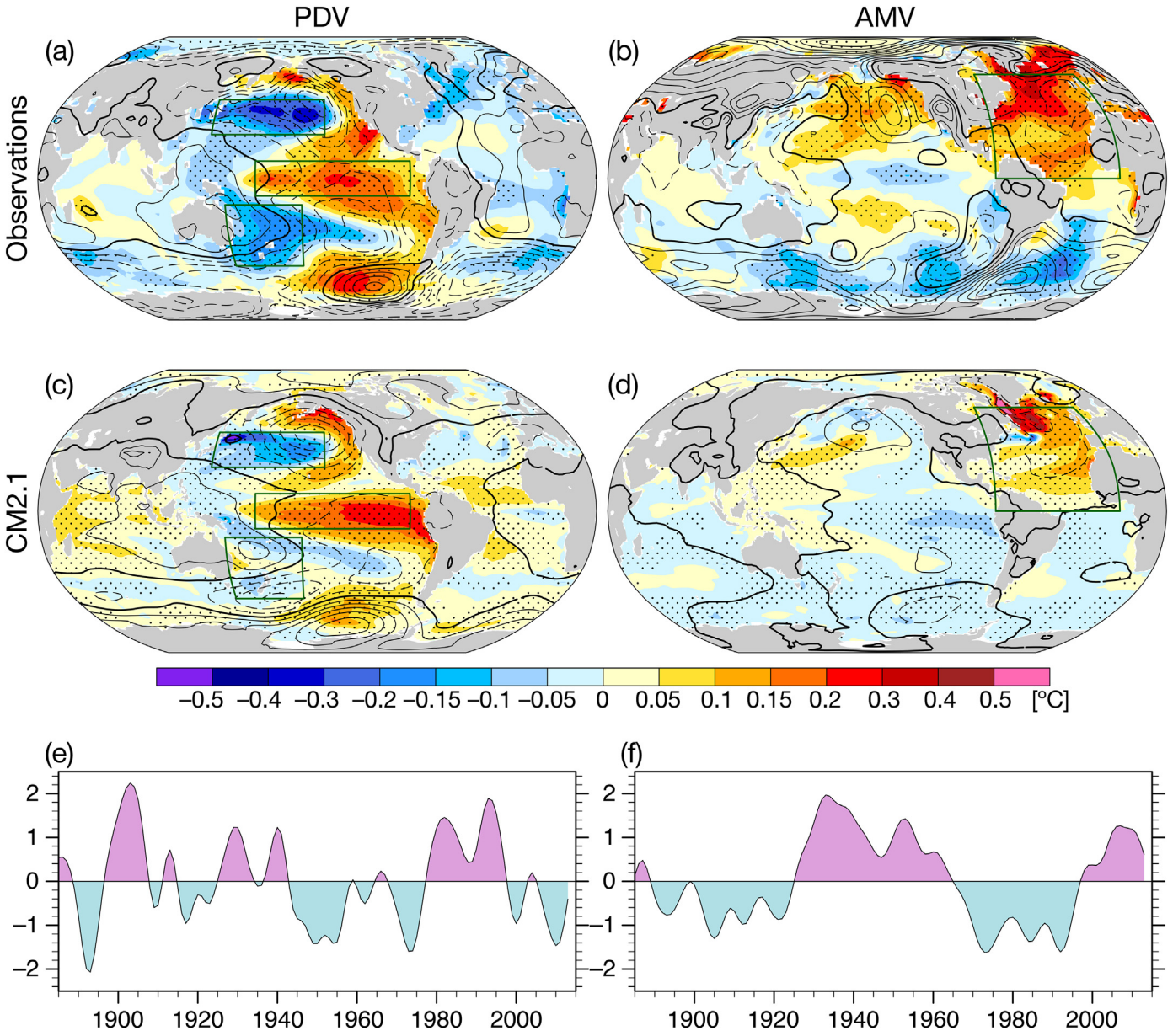

Fig. 1. Structures and historical evolutions of the PDV (left) and AMV (right). (a,b) Regressed anomalies of SST (shading) and SLP (contours for every 0.1 hPa; zero contour thickened) against the standardized (a) PDV index and (b) AMV index. The observed PDV and AMV index time series are shown in (e) and (f), respectively. The observed regressions and time series are based on SST of Extended Reconstructed SST version 5 (Huang et al., 2017) and SLP of NOAA 20th Century Reanalysis v2c (Compo et al., 2011) from 1880 to 2018 (SST) and 2014 (SLP). (c,d) As in (a,b) but based on a 700-year preindustrial control simulation by GFDL CM2.1. The PDV index is defined as SST* anomaly difference between the equatorial Pacific box and an average of the Northwest and Southwest Pacific boxes in (a, c), following Henley et al. (2015). The AMV index is defined as SST* anomalies in the North Atlantic box in (b, d), following Trenberth and Shea (2006). SST* indicates SST minus its global average. All results are obtained after annual averaging and applying a 10-year Lanczos low-pass filter.

Dong et al., 2014; Boo et al., 2015; Smith et al., 2016; Takahashi and Watanabe, 2016), and greenhouse gas forcing (Meehl et al., 2009; Lapp et al., 2012; Dong et al., 2014; Fang et al., 2014; Xu and Hu, 2018). The potential aerosol influence on the AMV (Section 2.2) and the aforementioned inter-basin influence from the Atlantic to the PDV suggest indirect external driving of the PDV. Yet, the impact of anthropogenic forcing on the PDV in the historical record is still unclear, as contrasting studies have suggested little influence (Si and Hu, 2017; Oudar et al., 2018), a negative PDV trend over the past four decades forced by anthropogenic aerosols (Allen et al., 2014), and a positive 20th century trend forced by the combined influence of greenhouse gases and anthropogenic aerosols (Dong et al., 2014). Based on the analysis of CGCM simulations, both Fang et al. (2014) and Xu and Hu (2018) conclude that the PDV will weaken and shift to a higher frequency in the 21st century under increasing greenhouse gases.

The current generation of coupled global climate models (CGCMs) successfully capture the spatial structure of the PDV (Henley et al., 2017). Fig. 1c presents an example based on a Coupled Model Intercomparison Project phase 3 (CMIP3) generation CGCM, the Geophysical Fluid Dynamics Laboratory CM2.1. The pattern similarity between the observed and simulated PDV demonstrates the ability of CGCMs to simulate the general PDV structure, although SST anomaly biases are found east of Japan where the model overshoots the Kuroshio current, and the simulated South Pacific signal is notably weaker than observed. These biases are common to the multi-model ensemble (MME) mean of CMIP5 models (Henley et al., 2017). The MME mean also features excessive westward extension of equatorial Pacific SST anomalies, which is related to the common negative cold tongue SST bias (Henley et al.,

2017). However, CM2.1 is not subject to that SST anomaly bias (Fig. 1c). Apart from the spatial features, CMIP5 models tend to underrepresent the magnitude of the PDV (Henley et al., 2017). The standard deviation of the PDV index for Fig. 1 is 23% weaker in CM2.1 compared to the observations. In CMIP5, this bias is related to overly biennial tendencies of ENSO (Kociuba and Power, 2015).

2.2. Atlantic multidecadal variability

A second leading pattern of internal multidecadal SST variability is focused in the tropical and North Atlantic regions. This mode, termed the "Atlantic Multidecadal Oscillation (AMO)" (Kerr, 2000) and more recently the AMV, features a dipolar SST pattern over the Atlantic, with the positive phase featuring positive SST anomalies in the tropical and North Atlantic, and negative SST anomalies in the South Atlantic (Fig. 1b). The observed time series features multidecadal periods of preferred phase, with the positive AMV phase dominating since about 1995 (Fig. 1f). As with the PDV, the broad range of frequencies rather than a single frequency over which the mode varies has resulted in some preferring the "variability" over "oscillation" terminology (Zhang, 2017; Sutton et al., 2018). The AMV has significant impacts on many climate phenomena of societal importance, including Sahel/Indian summer monsoon rainfall, Atlantic hurricanes, and summer climate over North America, Europe, and East Asia (e.g., Folland et al., 1986; Sutton and Hodson, 2005; Knight et al., 2006; Zhang and Delworth, 2006; Si and Hu, 2017; Yan et al., 2017), and also modulates some of the metrics of global climate change that are the focus of this review.

Several mechanisms are hypothesized to contribute to AMV. There has been recent debate regarding the contribution from external radiative forcing, particularly from anthropogenic aerosols (Booth et al., 2012; Zhang et al., 2013a; Si and Hu, 2017), but evidence increasingly supports the AMV as primarily arising through internal climate variability (Zhang et al., 2019c). Consistently, the CM2.1 simulation with fixed radiative forcing captures the basic structure of the AMV (Fig. 1d) though with some biases discussed briefly below. Some recent studies have suggested that AMV can arise from stochastic atmospheric forcing alone (Clement et al., 2015, 2016), but the degree to which this holds in nature has been questioned (Zhang et al., 2016; Kim et al., 2018b; Zhang et al., 2019c). Multiple lines of evidence instead support that AMV is strongly linked to internal variability of the Atlantic Meridional Overturning Circulation (AMOC) (Zhang et al., 2019c). Multidecadal variability in the AMOC and associated meridional heat transport are believed to be leading contributors of the AMV-related subpolar Atlantic SST anomalies. These SST anomalies propagate southward to the tropical Atlantic in a horseshoe pathway through coupled air-sea feedbacks, including wind-evaporation-SST feedback, cloud feedback, and dust feedback (Smirnov and Vimont, 2012; Wang et al., 2012a; Bellomo et al., 2016; Brown et al., 2016; Yuan et al., 2016; Amaya et al., 2017).

Several observational and modeling studies propose that AMV and PDV may be dynamically linked. Observational analyses suggest that the multidecadal component of the negative phase PDV lags the positive AMV by about a decade (d'Orgeville and Peltier, 2007; Zhang and Delworth, 2007), although the short observational record limits the confidence in this relationship. A potential causal link has been simulated in a CGCM with prescribed AMV-related surface heat flux anomalies that mimic the AMOC-induced changes in meridional heat transport (Zhang and Delworth, 2007). According to this study, enhanced Atlantic meridional heat transport associated with the positive AMV leads to reduced atmospheric meridional heat transport, and weakening of the storm track and Aleutian low, and thus warming of the western North Pacific through westward-propagating ocean Rossby waves. The reverse scenario is expected for the negative AMV phase. Additional studies have described a tropical pathway for an AMV and PDV link by which Atlantic warming induces strengthening of the trade winds, La Niña-like cooling in the eastern equatorial Pacific, and a weakened Aleutian low in the North Pacific (McGregor et al., 2014; Kucharski et al., 2016; Li et al., 2016; Ruprich-Robert et al., 2017). Therefore, AMV may be a source of predictability for PDV (Chikamoto et al., 2015).

Although state-of-the-art CGCMs are capable of simulating some facets of AMV, as with PDV, notable biases in AMV and related AMOC variability remain. Most CGCMs underestimate the amplitude of the unforced component of AMV (Kavvada et al., 2013; Park et al., 2016; Kim et al., 2018a; Yan et al., 2018). The CM2.1 representation of AMV (Fig. 1d) is consistent with this tendency, as the SST regression pattern is lower in amplitude than the observational counterpart in most regions, with the 46% weaker standard deviation of the AMV index (although the radiatively forced component is potentially aliased into the observational estimate). Most current CGCMs struggle to simulate realistic multidecadal AMOC variability and underestimate the linkage between AMOC variability and AMV (Yan et al., 2018).

3. GMST: The global warming staircase

GMST remains the most widely monitored metric of global climate change. Its importance is heightened by its prominence in proposed policies for climate change prevention and mitigation, as international agreements such as the United Nations Framework Convention on Climate Change Paris Agreement use specific GMST change targets as a basis for their structure. Global averaging for GMST has an advantage in robustness over regional temperature metrics, given that the spatial averaging eliminates regional contributions from internal climate variability, and so GMST trends are expected to emerge from the noise of internal climate variability more quickly than most regional temperature trends. Another attractive feature of GMST for monitoring climate change is long and relatively abundant instrumental records of surface air temperature and SST measurements.

The observed GMST time series since 1880 (Fig. 2, top) indicates a detectable upward trend that is attributable to anthropogenic influence (Bindoff et al., 2013). However, the GMST record also reveals wide variability across a range of timescales. On interannual timescales, GMST fluctuations are dominated by ENSO (Pan and Oort, 1983; Trenberth et al., 2002). Major volcanic eruptions, such as that of Mount Pinatubo in 1991, are linked with rapid cooling that persists for several years. On the multidecadal timescale, GMST increased steadily in the early 20th century from around 1910 to the 1940s, and the late 20th century from the 1970s to the late 1990s. These warming epochs are interrupted by two hiatus or slower warming epochs in the mid-20th and early-21st centuries.

This staircase-like GMST increase contrasts markedly with the purely externally forced warming as represented by the CMIP5 ensemble mean of the historical simulations, extended by a Representative Concentration Pathway (RCP) scenario (Fig. 2, middle). The simulated radiatively forced GMST time series features a rather smooth GMST increase devoid of the ENSO-related interannual variations. The increase slows from the 1950s to the 1960s due to increases in anthropogenic aerosols, followed by accelerated warming punctuated by temporary volcanically induced cooling from the 1960s to the present. However, the simulated GMST time series lacks a considerable amount of the observed decadal to multidecadal variability, including the recent hiatus.

As discussed in the introduction, the discrepancy between simulated and observed GMST motivated substantial scientific focus into its causes (Medhaug et al., 2017). These efforts resulted in major updates in observational GMST products (Karl et al., 2015; Hausfather et al., 2017) with elaborate infilling of areas with missing observations (Cowtan and Way, 2014), but the resulting adjustments still do not remove the apparent slowing of the GMST increase during the hiatus period. Instead, studies robustly identified the negative phase of PDV as the major driver of the hiatus. Having a similar SST anomaly pattern to ENSO, the PDV can modulate GMST on decadal time scales. Indeed,

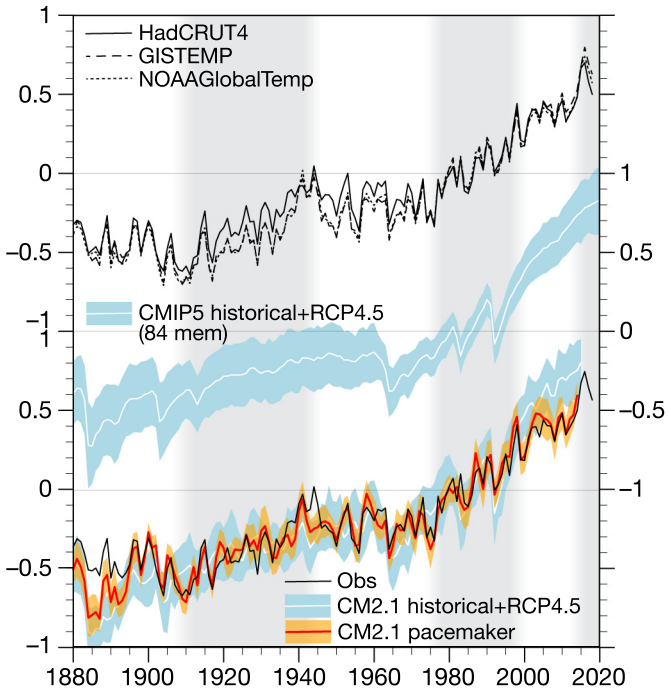

Fig. 2. GMST anomalies relative to 1970–1999 average. (top) Observations from HadCRUT4.6.0.0 (Morice et al., 2012), GISTEMP v4 (Lenssen et al., 2019), NOAAGlobalTemp version 5 (Zhang et al., 2019a). (middle) CMIP5 historical simulations extended with the RCP4.5 scenario by 84 members from 42 models. (bottom) CM2.1 20-member historical simulations extended with the RCP4.5 scenario (blue shading with a white curve), 10-member tropical Pacific pacemaker simulations (orange shading with a red curve), and average of the three observations shown at the top (a black curve). Rapid warming and hiatus/slow warming epochs are highlighted by grey and white backgrounds, respectively. For model simulations, the curve and shading indicate ensemble mean ± one ensemble standard deviation. For CMIP5 models, an anomaly is relative to 1970–1999 average of each ensemble member. For CM2.1, an anomaly is relative to 1970–1990 average of the ensemble mean of the pacemaker simulations. CM2.1 simulations are those used in Kosaka and Xie (2016).

studies have identified the PDV as the leading driver of internal GMST variability on decadal time scales in observations and CGCMs (Meehl et al., 2011, 2013; Maher et al., 2014; Middlemas and Clement, 2016). The PDV transition from positive (El Niño-like) to negative (La Niña-like) states in the late 1990s, and its persistence through the early 2010s, partially offset the radiatively-forced GMST increase. This is corroborated by the success of pacemaker simulations with CGCMs, where the PDV evolution is forced to follow observations but the simulations are freely evolving outside of a portion of the tropical Pacific, in reproducing the GMST hiatus (Kosaka and Xie, 2013; England et al., 2014; Watanabe et al., 2014; see Fig. 2, bottom). Additional contributions have been suggested from atmospheric internal variability in the winter Northern Hemisphere (NH) (Deser et al., 2017; Molteni et al., 2017) and volcanic aerosols from small eruptions (Santer et al., 2014).

The recent hiatus and the success of tropical pacemaker experiments has motivated researchers to revisit historical multidecadal GMST variability extending farther back in time. In particular, a long pacemaker simulation with SST anomalies restored toward observational values in the tropical Pacific in a CGCM reproduces the full warming staircase fairly well (Fig. 2, bottom). A notable discrepancy is found during World War II for which GMST and tropical Pacific SST observations are less reliable. Still, improvement from historical simulations is clear. The correlation coefficient of raw (quadratically detrended) GMST with the average of the three observational products for 1890–2014 is 0.93 (0.44) for the historical simulations and 0.97 (0.80) for the pacemaker simulations after ensemble averaging. Other pacemaker simulations with different CGCMs where momentum flux into the tropical Pacific Ocean is overridden by reanalysis values also reproduce the historical warming acceleration and slowdown (England et al., 2014; Svendsen et al., 2018).

The success of pacemaker simulations illustrates that the PDV is the key pacemaker of the staircase-like GMST increase, determining the timing of decadal warming acceleration and slowdown. Without the PDV influence, the early 20th century warming (~1910–1940) would have been much slower than the late 20th century warming, the mid-20th century hiatus would have ended in the mid-1960s as opposed to the 1970s in observations, and warming since the 1970s would have been more linear except for short drops induced by volcanic eruptions. The PDV's role is also supported by the spatial structure and seasonality of observed decadal surface temperature trends (Kosaka and Xie, 2016). Recent studies have demonstrated promise in generating skillful initialized predictions of Pacific decadal variability, including the notable PDV phase transitions and the associated changes in global and regional temperature (Meehl and Teng, 2012, 2014; Meehl et al., 2014, 2016c; Thoma et al., 2015). PDV predictability remains an active area of research. Some studies (e.g., Dai et al., 2015; Wu et al., 2019) also identified a role for AMV in modulating multidecadal GMST variability, but the PDV is generally regarded as a much bigger driver of the GMST staircase.

4. Earth's energy budget and climate feedbacks

The global warming hiatus also stimulated refinements in our understanding of climate feedbacks and GMST change from an energy theory perspective. Most notably, studies focused on recent observed GMST changes have challenged the notion that global climate feedbacks are the same for internal variability and long-term climate change, which sheds doubt on the ability to determine reliable estimates of climate sensitivity from short-term observational records. However, recent progress has illuminated sources of discrepancy between feedbacks operating on distinct timescales.

The energy view for GMST change relates the energy imbalance at the top of the atmosphere (TOA) (N, downward positive) to the radiative forcing (F) owing to, say, anthropogenic greenhouse gases and aerosols and to a climate feedback parameter (λ) that is approximated as proportional to GMST change (T)

$$N = F - \lambda T \tag{1}$$

The parameter λ incorporates well-known feedback processes that alter Earth's energy budget, including the Planck, lapse rate, water vapor, cloud, and sea ice/snow surface albedo feedbacks (e.g., Bony et al., 2006). The reciprocal, $s \equiv 1/\lambda$, is called the climate sensitivity parameter and provides the steady state global warming per unit of radiative forcing increase. Given that more than 90% of the energy added to the climate system is absorbed by the oceans (Trenberth and Fasullo, 2010; Von Schuckmann et al., 2016), the TOA radiation approximately balances the change in ocean heat content H ($dH/dt = N$).

The framework given by (1) has been supported extensively for long-term climate change (Gregory et al., 2004), but its application to the shorter-term changes, as with the hiatus, proved problematic. For (1) to apply to the global warming hiatus ($dT/dt = 0$), a substantial change in TOA radiation or an acceleration of ocean heat content change would be required, but neither is supported by the observational record (Levitus et al., 2012; Trenberth et al., 2014a; Loeb et al., 2012). Therefore, the Earth's energy budget given by (1) cannot be closed for the hiatus with realistic estimates of the budget terms.

Reconciling the energy theory and climate variability perspectives for the hiatus requires the consideration of distinct feedbacks for radiatively forced climate change and internal climate variability. Xie et al. (2016) demonstrated that TOA radiation and GMST are only weakly correlated for decadal and longer internal variability. They modified the energy theory of GMST change on decadal to climate

change timescales by decomposing the feedback into radiatively forced and internal change components

$$N = F - \lambda_F T_F - \lambda_I T_I, \quad (2)$$

where the subscripts F and I refer to forced and internal changes, respectively.

The reconciliation between the hiatus and energy view of GMST changes relates more generally to the enhanced focus of the dependence of the feedback parameter on timescale, and the ability to reliably estimate climate feedbacks and the related climate sensitivity from short observational records. Although some evidence suggested a reasonably strong correspondence between λ for both decadal and long-term climate change (Forster and Gregory, 2006), more recent studies noted that the differing patterns of surface temperature change between internal variability and climate change can result in distinct climate feedback and, therefore, climate sensitivity parameters (Colman and Power, 2010; Dalton and Shell, 2013; Dessler, 2013; Zhou et al., 2015; Gregory and Andrews, 2016; Xie et al., 2016; Zhou et al., 2016).

For the recent period between the 1980s and 2000s, which encompassed the hiatus period and was dominated by the negative phase of the PDV, evidence suggests that global mean cloud feedback is substantially more negative than the long-term cloud feedback (Zhou et al., 2016). This finding indicates that estimates of climate sensitivity derived from recent observational records would be biased low. The emerging physical explanation focuses on differences in surface temperature changes in regions of tropical ascent relative to those of tropical descent (Fig. 3). When warming is enhanced in the Indo-Pacific warm pool, such as in negative phase of the PDV but not for climate change, the enhanced tropical free tropospheric warming in response to moist adiabatic lapse rate adjustment tends to increase the inversion strength in regions of descent dominated by low cloud cover. This increase in inversion strength in those regions results in an increase in low cloud cover and a negative influence on the global cloud feedback (Zhou et al., 2016; Zhou et al., 2017; Andrews and Webb, 2018; Fig. 3b). In addition, the enhanced tropical free tropospheric warming relative to that of a pattern with less relative warming in the warm pool results in an enhanced lapse rate feedback, further contributing to a smaller climate sensitivity (Andrews and Webb, 2018). If relative warming instead is higher in regions of tropical and subtropical subsidence, then the opposite scenario is expected: inversion strength in subsidence regions weakens, low cloud cover diminishes, tropical free tropospheric warming is reduced, and both the global cloud and lapse rates feedbacks are more positive than in the warm pool-concentrated warming scenario.

Overall, these developments suggest weaker climate damping and higher climate sensitivity for the more spatially uniform surface warming pattern projected under global warming than for surface temperature change associated with the PDV. These recent findings emphasize the need to carefully consider the surface temperature trend patterns over the period for which climate feedbacks are estimated to determine if they are representative of long-term change, as important discrepancies may remain over multidecadal periods (Zhou et al., 2016; Xie, 2020).

These recent efforts also underscore that global ocean heat content (OHC) can be a more reliable indicator of the climate response to radiative forcing than GMST. TOA radiation imbalance does fluctuate in association with internal variability, as seen in fluctuations associated with ENSO (Loeb et al., 2012; Trenberth et al., 2015), but on decadal and longer time scales the TOA radiation anomalies due to internal variability become weaker (Xie et al., 2016) and the transient response to external forcing dominates. Consequently, internal variability of global OHC is also much weaker compared to GMST, even on multidecadal time scales (Palmer and McNeall, 2014; Fig. 4, top). This highlights that GMST is only weakly correlated with global heat accumulation due to external forcing and is not an ideal indicator to monitor climate change on decadal time scales.

The relationship between global OHC and GMST changes becomes complicated under aggressive GHG mitigations to slow global warming. Achieving low warming targets (GMST < 2 °C) as in the Paris Agreement requires deep emission cuts to reduce radiative forcing in the near future. Consider a scenario that stabilizes GMST by gradually reducing radiative forcing in time. Even when GMST levels off (starting in 2050 in RCP2.6, Fig. 5), TOA radiation remains positive and global OHC continues to increase ($dH/dt = N$), albeit at reduced rates (Long et al., 2019). In this scenario, global OHC fails to track the radiatively forced change in GMST, which presumably controls global surface climate change.

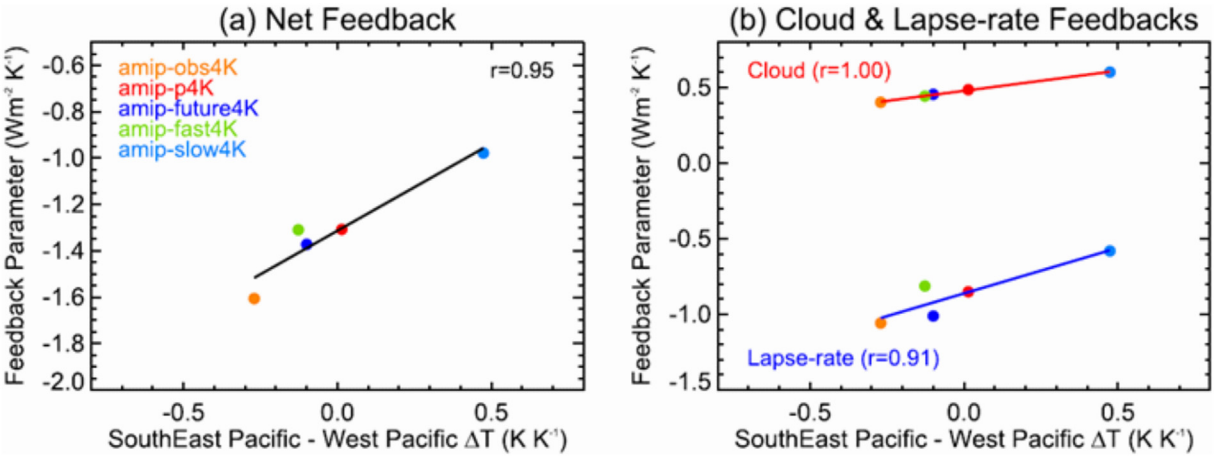

Fig. 3. Dependence of (a) net and (b) cloud and lapse-rate feedbacks on sea surface warming patterns. Feedbacks are determined through simulations of the Hadley Centre Global Environmental Model, version 2 and compared against control simulations forced with monthly observed SST and all forcing agents from 1979 to 2008. The perturbation experiments are the same as the control simulation but with perturbed SST forcing scaled to ensure a global-mean SST increase of 4 K and a warming pattern determined by: observed 20th century trends (amip-obs4K), uniform warming of 4 K (amip-p4k), CGCMs forced by a 1% yr-1 CO_2 increase (amip-future4k), years 1–20 (amip-fast4K) and years 21–150 (amip-slow4K) from CGCMs forced by an abrupt quadrupling of CO_2. The warming pattern (x-axis of each panel) is defined as the temperature change difference between the southeast tropical Pacific (30°S - 0°, 260°-280°E) and the west Pacific (15°S-15°N, 150°-170°E). Figure from Andrews and Webb (2018). © Copyright 15 January 2018 American Meteorological Society (AMS).

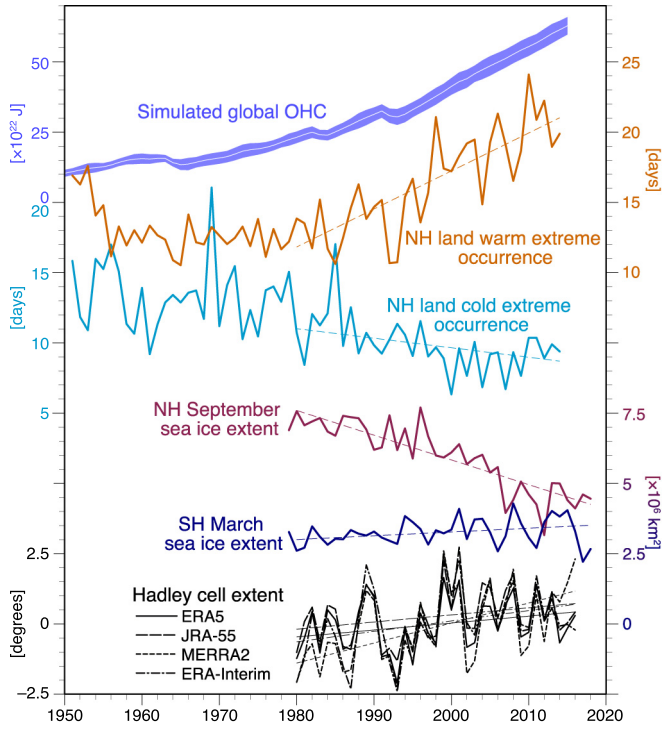

Fig. 4. Observed variability and change of global climate change metrics. (From top to bottom) Global OHC anomalies ($\times 10^{22}$J) in CM2.1 10-member historical simulations extended with the RCP4.5 scenario (white curve with blue shading). An anomaly is relative to 1901–1950 average of each ensemble member. The white curve and shading indicate ensemble mean ± one ensemble standard deviation. NH land warm (orange curve) and cold (light blue curve) extreme occurrences (days). See Fig. 8 for details. Observed sea ice extent in the September NH (purple curve) and March SH (navy blue) based on Version 3 of the National Snow and Ice Data Center (NSIDC) Climate Data Record of Passive Microwave sea ice concentration. Anomalies of annual mean Hadley cell extent relative to 1980–2016 based on reanalyses, evaluated as distance of NH + $SH_{\psi_{500}}$ = 0 latitudes (black curves). Straight lines superposed on the curves except global OHC show linear trends since 1980, evaluated as Sen's median slope.

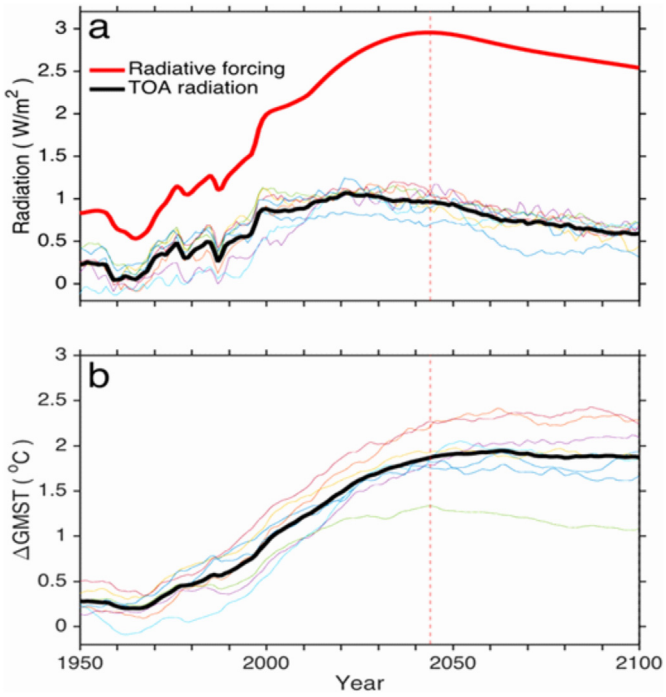

Fig. 5. Radiative forcing, TOA radiation *N*, and GMST change in RCP2.6 scenario. Eight CMIP5 models in thin lines and the ensemble mean in thick black lines. After 2050, GMST is nearly constant while TOA radiation continues to be positive (downward).

5. Polar amplified warming and sea ice changes

5.1. Understanding and attribution of the recent Arctic warming

Although the global warming hiatus indicated an apparent slowdown in GMST rise, one of the most robust climate changes induced by GHG warming, Arctic warming and the associated sea ice decline, continued unabated. Indeed, the fastest rate of warming has occurred in and around the Arctic (Serreze and Barry, 2011; Vaughan et al., 2013). A dramatic reduction in Arctic sea-ice cover and melting of Greenland ice sheet (GrIS) in the past decades are perhaps the most iconic symbols of global warming. Many processes and positive feedbacks contribute to polar amplified warming. Sea ice reduction initially triggered by anthropogenic forcing amplifies warming in the Arctic through sea ice-albedo and other positive feedbacks (Serreze et al., 2009; Screen and Simmonds, 2010a, 2010b). Other radiative and dynamical processes are also suggested to be sensitive to anthropogenic forcing and may have contributed to the warming process. These include cloud cover (Francis and Hunter, 2006; Kay et al., 2008; Choi et al., 2014) and water vapor changes in the high latitudes (Alexeev et al., 2005; Graversen and Wang, 2009; Zhang et al., 2013b), the warming effect of the strengthening surface thermal inversion (Bintanja et al., 2011), increases in soot on snow (Hansen and Nazarenko, 2004) and heat-absorbing black carbon aerosols in the atmosphere (Shindell and Faluvegi, 2009), increases in northward atmospheric transport (Graversen et al., 2008; Yang et al., 2010; Lee, 2012), and ice and oceanic dynamics and heat transport (Bengtsson et al., 2004; Woodgate et al., 2006; Shimada et al., 2006; Chylek et al., 2009; Zhang, 2015; Polyakov et al., 2017).

Although CGCMs simulate most of these mechanisms that amplify polar warming, the rate of observed Arctic warming and sea ice loss over the past 40 years exceeds the response to increased anthropogenic forcing according to these CGCMs (Stroeve et al., 2012; Notz and Stroeve, 2016). This discrepancy has stimulated research into possible deficiencies in simulating the forced polar warming as well as possible sources of internal climate variability that may be responsible for this difference. Internal drivers of sea-ice variability have been suggested to originate from both oceanic (Zhang, 2015; Tokinaga et al., 2017) and atmospheric processes (Ding et al., 2017; Olonscheck et al., 2019). The AMV and the PDV were both suggested to be major internal drivers of Arctic surface temperature and sea-ice variability via their related oceanic and atmospheric heat transport on multidecadal timescales (Zhang, 2015; Chylek et al., 2009; Screen and Francis, 2016). Recent studies have revealed that tropical SST variability exerts significant impact on Arctic climate (Ding et al., 2014, 2019; Screen and Deser, 2019; Meehl et al., 2018). The negative PDV phase has contributed to a strong positive geopotential height trend near Greenland, via generation of a large-scale wave train extending from the equatorial Central and Eastern Pacific to the Arctic (Ding et al., 2019; Baxter et al., 2019). This localized circulation trend in the North American sector of the Arctic has favored strong regional warming that has reinforced the anthropogenic warming trend in the Arctic. This anomalous high-pressure trend can also cause strong subsidence over the Arctic Ocean and Greenland, which adiabatically warms the atmosphere above the sea ice and land ice. At the same time, increases in moisture advection and cloudiness are driven by an anomalous anticyclonic circulation pattern centered over Greenland. This combination of a warmer, cloudier, and more humid atmosphere increases downward longwave radiation and leads to increases in sea ice and GrIS melt, and SST warming in high latitudes (Ding et al., 2019). Additionally, Meehl et al. (2018) suggests that the SST warming trend in the tropical Atlantic

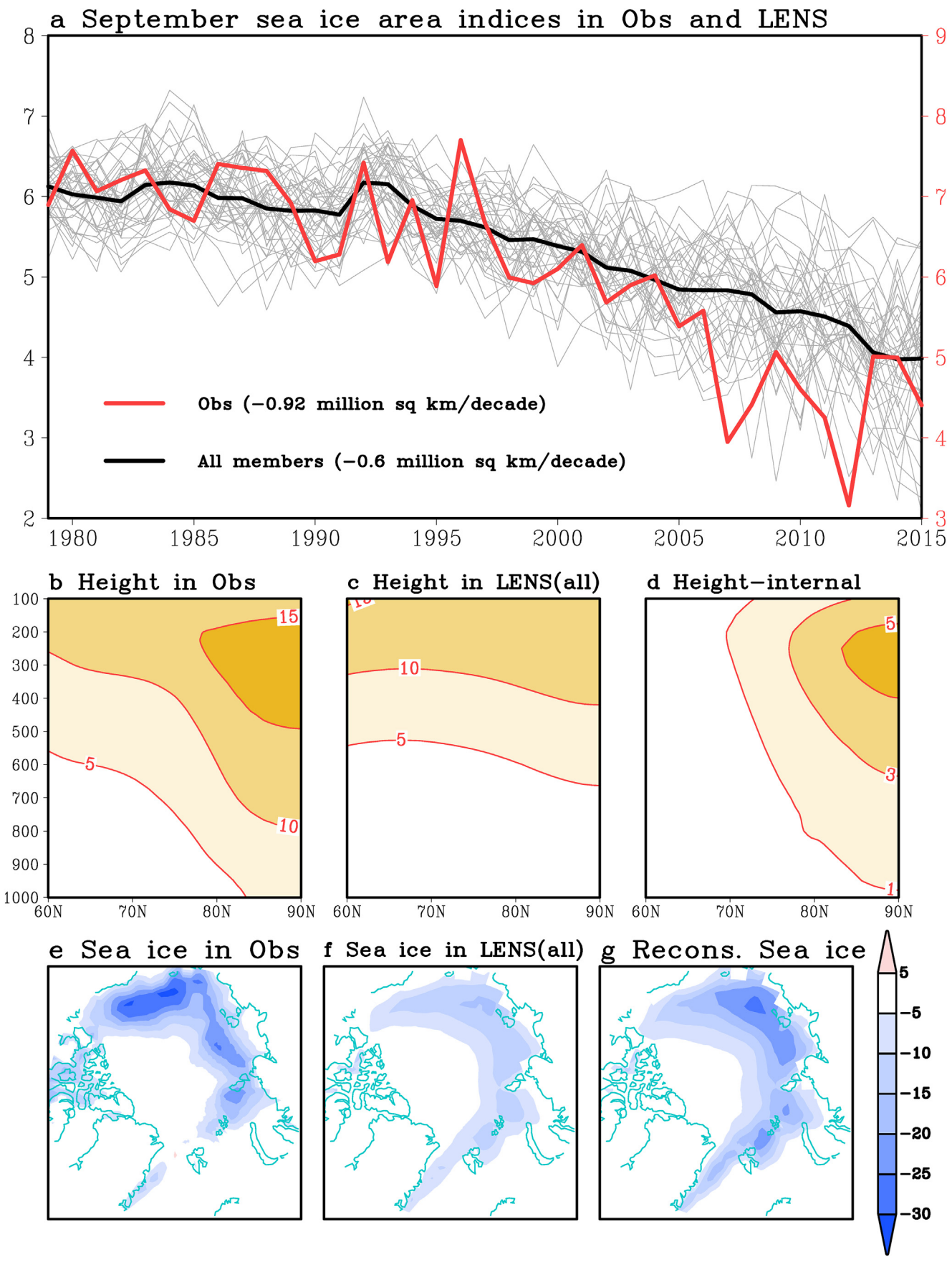

(caption on next page)

Fig. 6. September Arctic sea ice variability in observations and the Community Earth System Model Large Ensemble (LENS; Kay et al., 2015) from 1979 to 2015. (a) Total area of September sea ice extent in 40 members of the LENS (grey line) and National Snow and Ice Data Center (NSIDC) observations (red line) (unit: million km^2). The black curve represents the 40-member ensemble mean. Note that the right ordinate axis (in purple), corresponding to observed sea ice change, is shifted downward by one unit to align with the ensemble mean change, but the relative scales for the simulated and observed sea ice extent are the same. (b-d) Linear trends in June–August (JJA) zonal mean height (in m per decade), for the period 1979–2015: (b) observed (ERA-Interim reanalysis), (c) the 40-member LENS ensemble mean, and (d) the fast-minus-slow difference of JJA zonal mean height in the LENS. The difference in (d) is divided by 2 to approximate the deviation from the ensemble mean. The two JJA circulation patterns (c and d) were used in a fingerprint method (Ding et al., 2019) to represent atmospheric forced and internal drivers of September sea ice variability. By matching a linear combination of these two patterns with the observed counterpart (d), we can quantify the relative contribution of each forcing in causing total September sea ice variability over the period that is revealed in (e). e) Linear trends (% per decade) of September sea ice extent from the NSIDC passive microwave monthly sea ice record (1979–2015). f) the ensemble average of 40 members of the LENS. g) Reconstructions of September sea ice use the internal and forced modes derived from the fingerprint method described above. Figure adapted from Ding et al. (2019).

from 2000 to 2014 may drive a teleconnection that melts summer sea-ice through the wind drift effect.

Overall, as with the hiatus in GMST, these recent studies increasingly support that much of the discrepancy between the observed and simulated Arctic warming and sea ice decline can be attributed to internal climate variability. Specifically, current estimates suggest that about 30–50% of the observed September Arctic sea ice decline is due to internal variability (Stroeve et al., 2012; Kay et al., 2011; Zhang, 2015; Ding et al., 2017, 2019). Because the fingerprints of internal variability and radiative forcing on Arctic atmospheric circulation trends are quite distinct, and because Arctic circulation exerts a strong influence on multidecadal Arctic sea ice trends, Ding et al. (2019) successfully reconstructed a substantial fraction of the observed Arctic sea ice extent trends as a linear combination of internal and radiatively forced components (Fig. 6). To the extent that this internal variability is rooted in the tropical Pacific processes (Lee et al., 2011; Ding et al., 2014), both the GMST slowdown and accelerated Arctic warming may have similar origins; the tropical Pacific cooling slows the forced rising trend in the case of GMST but enhances the forced trend in the case of Arctic warming.

5.2. Understanding and attribution of recent Antarctic climate variability

In contrast to the broad warming and sea ice melting trends in the Arctic, recent atmospheric and surface temperature changes over the Antarctic exhibit strong regional and seasonal dependence with significant warming over the West Antarctic and the Peninsula region in winter and spring (Nicolas and Bromwich, 2014). Over most of East Antarctica, the temperature trend is not significant since 1979. Most surprisingly, the area covered by sea ice in the Antarctic exhibits a slight increasing trend from 1979 to 2014 that ended with a sudden drop in 2016 (Stuecker et al., 2017; Meehl et al., 2019; Fig. 7a), and SSTs in the Southern Ocean (SO) encircling the continent show cooling trends in the past three to four decades (Marshall et al., 2014, 2015; Armour and Bitz, 2015; Armour et al., 2016; Meehl et al., 2016a; Purich et al., 2016; Zhang et al., 2019b). The sea ice increase and SO cooling and mixed trends of temperature changes in the Antarctic are puzzling, because from energy balance considerations, increased greenhouse gases should have led to temperature warming and decreased sea ice extent (Fig. 7c) in the high latitudes of both hemispheres (Maksym et al., 2012).

Several mechanisms have been suggested to explain why the Antarctic cryosphere behaves so differently from its northern counterpart (Marshall et al., 2014, 2015). Anthropogenic forcing due to increased CO_2 and SH high-latitude ozone depletion are thought to be the primary drivers of the trends in Antarctic circulation (Thompson and Solomon, 2002; Fogt et al., 2009), which features a poleward shift of the jet stream that projects onto the positive phase of the Southern Annular Mode (SAM, Thompson and Wallace, 2000) in SH summer. It has been suggested that the strengthening of the circumpolar westerlies associated with the positive SAM trend has cooled Antarctica and, thus, increased the sea ice extent along the coast (Goosse et al., 2009). However, this explanation is debatable (Turner et al., 2009; Sigmond and Fyfe, 2010) and some model simulations driven by recent CO_2 increase and ozone depletion (Bitz and Polvani, 2012; Smith et al., 2012) show sea ice, SST and land surface temperature responses that are opposite to the observations; still others suggest that the simulated response of sea ice depends on the length of the time taken for the ocean to respond to anthropogenic forcing (Marshall et al., 2014, 2015). Another school of thought suggests that the high latitudes of the SH should be the last place on the planet to respond to global warming because the climatological meridional transport of surface water away from the continent can cool the SO surface by pumping unmodified water up from the deep ocean (Marshall et al., 2014, 2015; Armour and Bitz, 2015; Armour et al., 2016). Multiple factors can stabilize the upper part of the SO and limit the heat mixing into the deep water (Kirkman and Bitz, 2011).

In addition, some studies (e.g., Ding et al., 2011, 2012; Ding and Steig, 2013; Meehl et al., 2019) suggest that multi-decadal variability in the tropics may also play an important role for Antarctic climate. Temperature trends in West Antarctica and the Antarctic Peninsula can be well explained by trends in the high-latitude atmospheric circulation over the South Pacific Ocean mediated by barotropic Rossby waves due to the trend in tropical Pacific and Atlantic SSTs. Several studies reveal PDV- and AMV-related SST modes in the tropics that can exert a strong impact on the Pacific sector of Antarctica on decadal to multidecadal time scales. This tropical-related circulation trend may also influence the upper-ocean current and sea ice conditions along the coast of West Antarctica and the Peninsula region. These influences can well explain the recent increase of sea ice area around Antarctica (Li et al., 2014; Meehl et al., 2016a; Purich et al., 2016) and, in combination with other tropical and high-latitude climate variability, also may have contributed to the sudden decline in 2016 (Meehl et al., 2019).

5.3. Arctic and Antarctic warming during the early 20th century

Observations in the last 30 years reveal the importance of internal climate variability in shaping decades-long climate anomalies in the Arctic and Antarctic. Some suggest that the recent changes in the Arctic and Antarctic are not unparalleled in the past 100 years. From the 1910s to the 1940s, the Arctic experienced significant warming that is comparable to the recent 30-year warming (Johannessen et al., 2004; Bengtsson et al., 2004; Grant et al., 2009; Wood and Overland, 2010; Yamanouchi, 2011; Brönnimann, 2009). Several hypotheses were proposed for this early twentieth century warming, including external radiative forcing and internal climate variability. Some studies suggest increased solar radiation, decreased volcanic aerosols, and raising black carbon aerosols as key factors (Overpeck et al., 1997; Fyfe et al., 2013). However, most climate models driven by historical radiative forcing fail to simulate the early Arctic warming (Bengtsson et al., 2004; Semenov and Latif, 2012; Jones et al., 2013; Wegmann et al., 2017). Another explanation is internal low-frequency atmospheric variability, which can generate substantial interdecadal variability in long-term climate model control simulations (Johannessen et al., 2004). Furthermore, observational analyses by Wood and Overland (2010) and Yamanouchi (2011) suggest that the atmospheric circulation around Greenland in the last 100 years is dominated by interdecadal variability with another prominent rise in the 1930s–1940s. A possible cause of this multi-

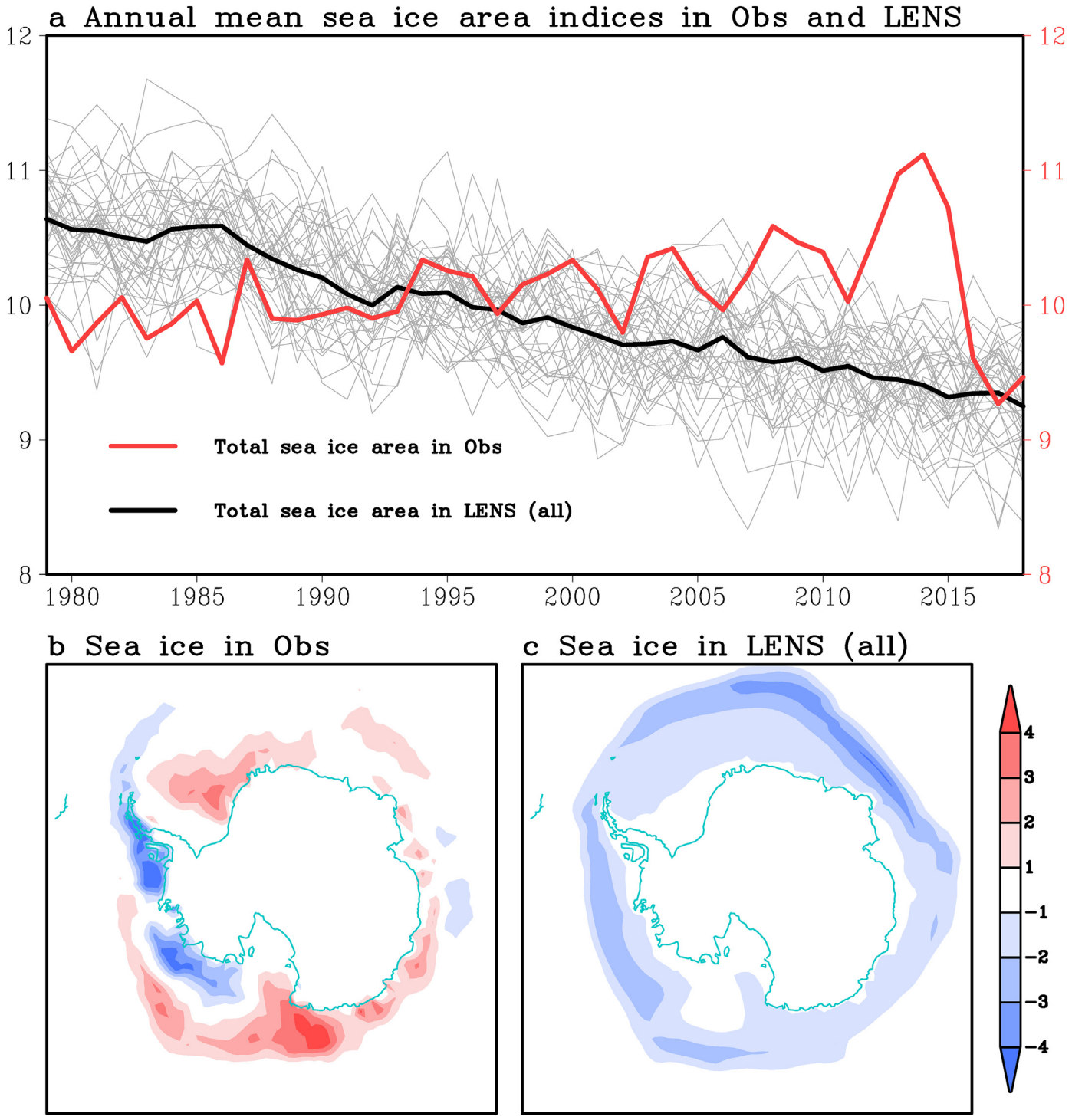

Fig. 7. Annual mean Antarctic sea ice variability in observations and the LENS from 1979 to 2018. a) Total area of annual mean sea ice extent in 40 members of the LENS (grey line) and NSIDC observations (red line) (unit: million km^2). The black curve represents the ensemble mean of 40 members. b) Linear trends (% per decade) of annual mean sea ice extent from the NSIDC sea ice record (1979–2018) and c) the 40-member LENS ensemble mean.

decadal circulation variability is interactions of the Arctic with low and mid-latitude regions (e.g., Polyakov et al., 2010).

More recently, both PDV and AMV have been suggested to be important for the early Arctic warming (Tokinaga et al., 2017; Svendsen et al., 2018). Both dominant interdecadal variability modes concurrently shifted from a negative to a positive phase in the mid-1920s, strengthening warm advection into the Arctic through changes in atmospheric circulation. Models forced by these interdecadal SST/surface wind changes successfully simulate the early Arctic warming. The most plausible answer to the earlier warming in the Arctic is a combination of intrinsic internal climate variability and positive feedbacks that amplified radiative and atmospheric forcing.

In the Antarctic, a warming period was also observed from the 1920s to 1940s in several ice core and ocean sediment core records (Schneider and Steig, 2008; Smith et al., 2017). However, few studies have investigated the causes of this early warming period. Tropical SST variability was suggested to be the most important forcing for this early 20th-century warming because CO_2 and ozone forcing was largely

muted during that period (Schneider and Steig, 2008; Smith et al., 2017). Over the Southern Ocean, the SST variability (Fan et al., 2014) seems to be out-of-phase with temperature changes in and around the Arctic over the past 50 years on low-frequency timescales. However, how robust this bipolar contrast between SST changes in the Southern Ocean and the temperature changes in the Arctic in a longer time period remains an open question.

6. Increasing warm and cold extreme occurrences

Since at least the beginning of the 20th century, Earth's land areas have experienced a significant increase in hot extreme occurrences and a decrease in cold extreme occurrences (Donat et al., 2013). Anthropogenic forcing is very likely a contributor to these changes since the mid-20th century (Bindoff et al., 2013). The global warming hiatus revealed, however, that these changes also may be interrupted, at least temporarily, by multidecadal periods for which the behavior of global land temperature extremes may be inconsistent with long-term trends and with GMST changes. Moreover, the behavior may vary substantially across seasons. Despite the nearly steady GMST during the hiatus, summertime hot extremes over land continued to increase without any evidence of a pause (Seneviratne et al., 2014; Su et al., 2017; Johnson et al., 2018), whereas wintertime cold extremes also increased during this period (Cohen et al., 2014; Sillmann et al., 2014; Johnson et al., 2018).

The contrasting behavior noted above suggests that the drivers of multidecadal extreme temperature changes over land differ from the dominant drivers of GMST and vary across seasons. In order to determine the factors influencing these recent changes, Johnson et al. (2018) developed an empirically based linear regression model that captures more than 75% of the variance of the observed summertime (June – September) warm extreme occurrences and wintertime (December – March) cold extreme occurrences over NH land, where extreme temperature occurrence is defined by daily maximum temperature falling below the 10th percentile or above the 90th percentile of the climatological distribution. In contrast with regression models for GMST (Lean and Rind, 2008; Foster and Rahmstorf, 2011), the models that successfully capture most of the variance of land temperature extreme occurrences require the influence of modes of climate variability in addition to ENSO.

For wintertime cold extreme occurrences, a large-scale "warm Arctic/cold continents" (WACC) pattern (Overland et al., 2011; Cohen et al., 2014) resembling the negative phase of the North Atlantic Oscillation or Arctic Oscillation was found to be critical for explaining the increase in cold extreme occurrences during the hiatus period. This pattern, identified in the 500 hPa geopotential height field and termed the "z500 extremes pattern," features height anomalies concentrated over the North Atlantic and Eurasia, with positive anomalies over the high latitudes and negative anomalies over the midlatitudes (Fig. 8a). The z500 extremes pattern represents the height pattern that explains the most wintertime cold extreme occurrence variance over NH land, after linearly removing the effects of the trend, ENSO, and volcanic aerosols (Johnson et al., 2018). The occurrence of this WACC height pattern is associated with increased cold extreme occurrences over North America and especially over Eurasia (Fig. 8c), indicating that the recent increase in hemispheric cold extreme occurrences is closely linked with a general wintertime Eurasian cooling (Cohen et al., 2012, 2014; Trenberth et al., 2014a, 2014b; Li et al., 2015; Deser et al., 2017). The increased frequency of the z500 extremes pattern over the past couple of decades has counteracted the long-term downward trend of NH land cold extreme occurrences, resulting in an overall increase during the hiatus period (Fig. 8e).

The corresponding analysis for summertime warm extreme occurrences revealed that an SST rather than 500 hPa geopotential height pattern played a leading role in explaining multidecadal extreme temperature variability. This SST pattern (Fig. 8b), which resembles the warm phase of AMV and referred to as the "SST extremes pattern," reinforced the long-term upward trend during the hiatus (Fig. 8f). The emergence of a pattern focused in the Atlantic contrasts the Pacific-centered PDV that has been the focus of multidecadal GMST variability (Section 3). The influence of the SST extremes pattern on warm extreme occurrences is focused over southeastern North America, central and eastern Europe, and Southeast Asia (Fig. 8d), a pattern that is consistent with AMV influence on seasonal mean temperature (Sutton and Hodson, 2005; Ruprich-Robert et al., 2017).

The identification of these two distinct modes of variability for modulating hemispheric land extreme temperature occurrence highlights that regional-scale temperature changes of greatest societal consequence may not track annual GMST closely, which underscores the limited usefulness of annual GMST as a measure of the state of the climate. Anomalous extreme temperature variability over continental regions, which mirrors the patterns of seasonal mean temperature anomalies (Johnson et al., 2018), are dominated by distinct modes of variability from those of GMST that vary seasonally. As seen during the hiatus period, the combined influence of the wintertime z500 extremes and summertime SST extremes patterns may result in multidecadal periods when both wintertime cold and summertime warm extreme occurrences over land increase simultaneously.

Although internal climate variability remains a likely culprit to explain a substantial amount of extreme temperature variability related to the WACC-like z500 and AMV-like SST extremes pattern, the possible role of anthropogenic forcing in modulating these modes of variability remains an area of intense scientific interest and debate. Regarding the recent prevalence of the WACC pattern, the debate focuses on the possible impact of polar amplified warming and Arctic sea-ice loss (Overland et al., 2011; Francis and Vavrus, 2012; Cohen et al., 2014; Barnes and Screen, 2015; Kug et al., 2015; Li et al., 2015; McCusker et al., 2016; Sun et al., 2016; Ogawa et al., 2018; Koenigk et al., 2019), especially in the Barents-Kara Seas region (Honda et al., 2009; Petoukhov and Semenov, 2010; Inoue et al., 2012; Kim et al., 2014; Mori et al., 2014; Zhang et al., 2018a). Disagreements are rooted in the incomplete knowledge of the mechanisms that may link Arctic sea ice loss and midlatitude cooling, with hypotheses suggesting both tropospheric (e.g., Alexander et al., 2004; Magnusdottir et al., 2004) and stratospheric (e.g., Kim et al., 2014; Zhang et al., 2018a) pathways, and inconsistencies among climate models in simulating the wintertime midlatitude temperature response to Arctic sea ice loss, which includes important dependencies the choice of atmosphere-only or fully coupled simulations (Deser et al., 2016; Screen et al., 2018) and sufficient vertical resolution to simulate possible stratospheric pathways (e.g., Zhang et al., 2018a). Johnson et al. (2018) found a statistically significant link between negative boreal autumn Barents-Kara sea ice anomalies and the enhanced wintertime occurrence of the z500 extremes pattern in observations, but confidence in a physically meaningful link requires additional lines of evidence. Through an analysis of surface turbulent heat fluxes associated with sea ice loss in observations and CGCMs, Blackport et al. (2019) suggest that both reduced sea ice and recent cold midlatitude winters are driven by atmospheric circulation, indicating that reduced cold midlatitude winters are coincident with but not caused by reduced Arctic sea ice. Cohen et al. (2020) provide a more thorough review of the challenges in deciphering the role of Arctic amplification in midlatitude severe winter weather, particularly with respect to diverging conclusions from observational and climate modeling studies, while also noting that converging scientific evidence and ideas may allow consensus to emerge in some facets of this problem.

The AMV-like SST extremes pattern, which captures the nonlinearity in the warm extreme temperature occurrence trend (Fig. 8f), also may reflect, in part, an influence from anthropogenic forcing, as discussed in Section 2.2. Evidence indicates that North Atlantic cooling induced by anthropogenic aerosols projects onto observed AMV (Mann and Emanuel, 2006; Villarini and Vecchi, 2013), and so care must be

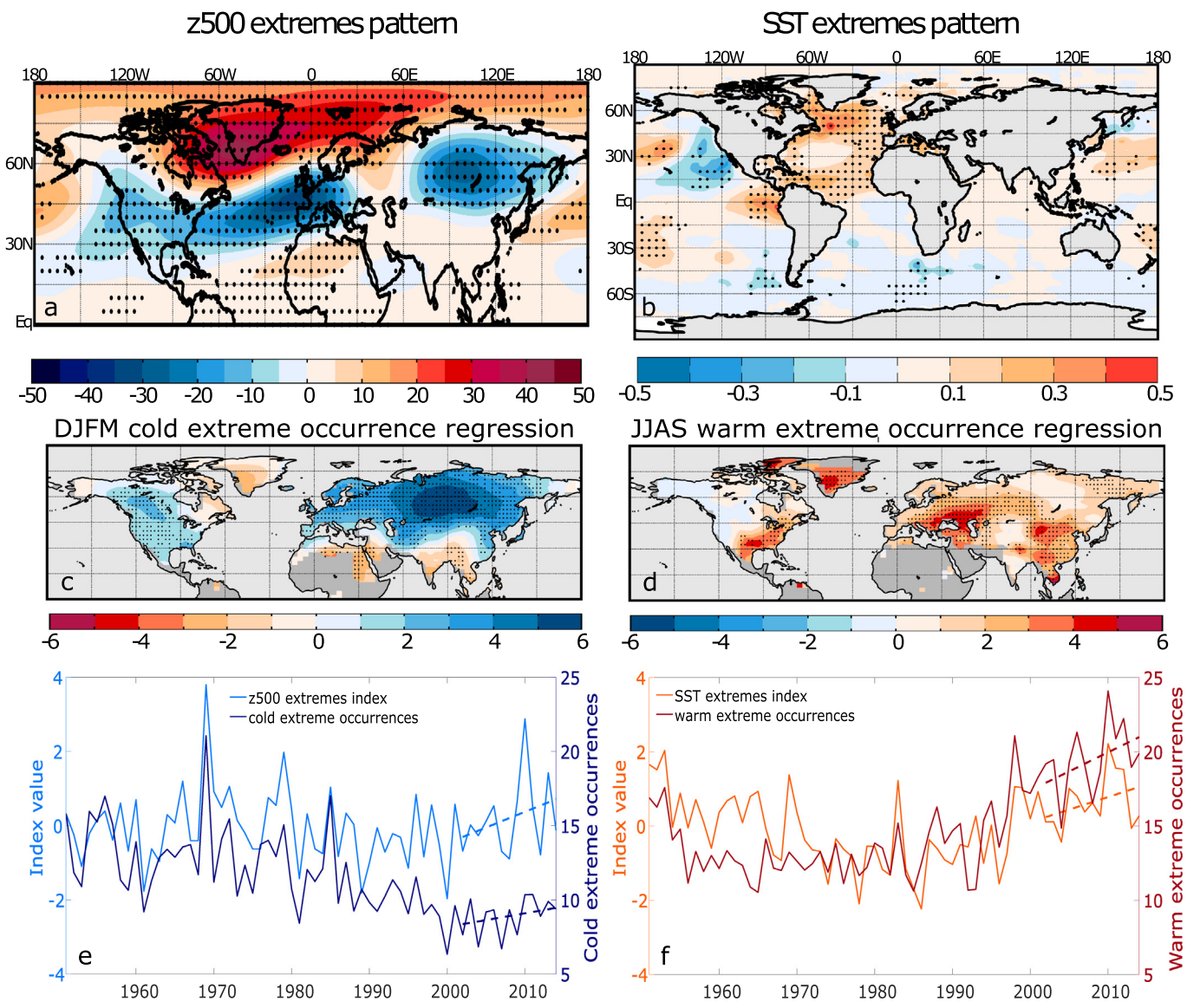

Fig. 8. Dominant climate patterns modulating extreme temperature occurrence over Northern Hemisphere land. a) Partial regression coefficients of 500 hPa geopotential height on the z500 extremes pattern index time series (m per standard deviation) for December – March (DJFM), where the z500 extremes pattern is defined as the 500 hPa geopotential height pattern that explains the most Northern Hemisphere land cold extreme temperature occurrence after linearly removing the influence of ENSO, trend, and volcanic aerosols (Johnson et al., 2018). Stippling indicates regression coefficients that are significant at the 5% level based on an F-test. Extreme occurrence data (below the 10th or above the 90th percentile of the temperature distribution) are based on HadEX2 data (Donat et al., 2013) through 2010 and ERA-Interim (Dee et al., 2011) after 2010. b) As in a) but for the partial regression of SST anomalies on the June–September (JJAS) SST extremes pattern (Johnson et al., 2018). c) Partial regression of December–March cold extreme occurrences (days) on the z500 extremes pattern time series and of d) June–September warm extreme occurrences on the SST extremes pattern time series. e) 1951–2014 time series of December–March cold extreme Northern Hemisphere land cold extreme occurrences (days; dark blue and right y-axis) and the z500 extremes pattern index (light blue and left y-axis). Dashed lines indicate the 2002–2014 linear trend lines. The correlation coefficient between the two time series is 0.52. f) As in e) but for the June–September warm extreme occurrences (red and right y-axis) and the SST extremes pattern index. The correlation coefficient between the two time series is 0.56.

taken to distinguish internal from forced AMV (Mann et al., 2014; Ting et al., 2014; Si and Hu, 2017). However, a large fraction of AMV likely is internally generated (Zhang et al., 2019c), potentially contributing to the apparent acceleration of sea surface warming in the late 20th and early 21st centuries (Delsole et al., 2011) and, by extension to the analysis above, of summertime warm extreme temperature occurrence over NH land. The SST extremes pattern emerged as a leading pattern of summertime extreme temperature occurrence variability, after removing the effects of ENSO, in a 500-yr coupled GCM simulation with constant radiative forcing (Johnson et al., 2018). These lines of evidence support the existence of an AMV-like SST extremes pattern as a naturally occurring pattern that can induce apparent accelerations or decelerations of the warm extreme occurrence trend over land.

7. Hadley cell expansion

Another robust climate response to human activity is the poleward expansion of the Earth's subtropical dry zones. These arid regions are centered at roughly 30°S and 30°N and result from dynamics associated with a pair of global-scale circulations—the Hadley cells. Within the tropics, the Hadley cells dominate zonal mean atmospheric circulation, with moist convection in the deep tropics (e.g., the Intertropical Convergence Zone, ITCZ), poleward flow aloft, dry subsidence in the subtropics, and equatorward flow near the surface. Subtle shifts in the poleward extent of the descending branches, in particular, can have profound impacts on surface hydrology over land (Hoerling et al., 2012; Ye, 2014; Zhang and Delworth, 2018). Therefore, understanding

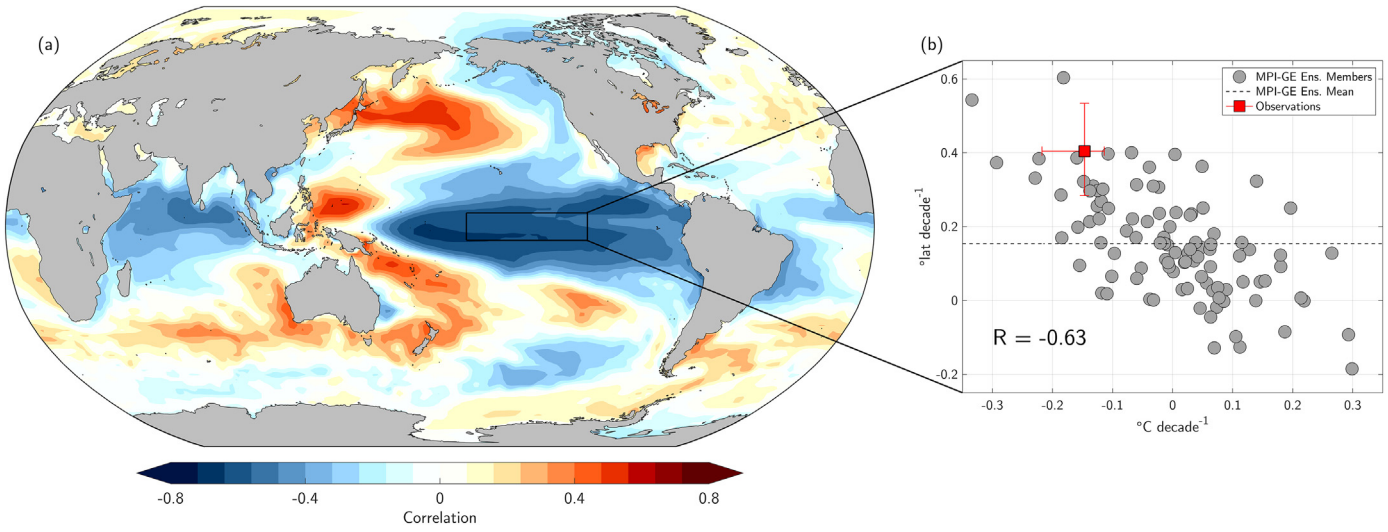

Fig. 9. Relationship between Hadley cell expansion/contraction and Pacific sea surface temperatures. **(a)** Correlation (shading) of 100 total (NH + SH) $\psi_{500} = 0$ trends with 100 SSTA* trends at each grid point using MPI-GE from 1985 to 2014. **(b)** Scatter plot of total $\psi_{500} = 0$ trends (y-axis; °latitude decade^{-1}) and SSTA trends averaged in the Niño3.4 region (x-axis; °C decade^{-1}). Grey circles represent trends derived from MPI-GE. Dashed black line indicates MPI-GE total $\psi_{500} = 0$ ensemble mean. Note that MPI-GE Niño3.4 trends are relative to the ensemble mean (i.e., Niño3.4*). Red box and whiskers represent the median and range, respectively, of trends derived from observed products. Observed total $\psi_{500} = 0$ trends calculated using ERA-Interim, ERA5, MERRA2 (analyzed), and JRA-55. Observed Niño3.4 trends calculated using ERSSTv3b, ERSSTv5, HadISSTv1.1, and ICOADS.

Hadley cell edge variability and its forced trends is of great socio-economic concern and has been a major focus of recent scientific inquiry.

In response to GHG increase, theoretical and modeling studies indicate a widening and weakening of each hemisphere's Hadley cell (Lu et al., 2008; Staten et al., 2012; Tao et al., 2016). The precise dynamical mechanisms governing GHG-induced Hadley cell expansion are still an open research question (Staten et al., 2018); however, the literature has highlighted the importance of forced changes in subtropical static stability (e.g., Lu et al., 2008) and the equator-to-pole temperature gradient (Wittman et al., 2007; Lorenz, 2014) across the tropopause in determining the meridional location and intensity of breaking mid-latitude eddies, which are thought to significantly contribute to the descending motion of the Hadley cell via the so-called “eddy-pump” effect (Robinson, 2002; Walker and Schneider, 2006). Other anthropogenic contributions to Hadley cell expansion arise from stratospheric ozone depletion over Antarctica (e.g., Polvani et al., 2011) and the atmospheric heating effects of aerosols such as black carbon and tropospheric ozone (Allen et al., 2012).

What role does anthropogenic climate forcing play in observed Hadley cell expansion in recent decades and to what extent do observed trends deviate from the expected external forcing? The best estimates using modern reanalysis data show that each zonal mean Hadley cell is expanding at a rate of ~0.1–0.5° latitude decade^{-1}, with the SH cell currently outpacing its NH counterpart (Staten et al., 2018). However, climate models forced with the aforementioned anthropogenic radiative forcings produce expansion trends on the lower end of the observed range (~0.1° latitude decade^{-1}), suggesting that external forcing alone cannot explain the observations.

As with the other metrics discussed in previous sections, growing evidence has pointed to the primary importance of internal climate variability for explaining the faster than expected Hadley cell expansion. It has long been established that El Niño (La Niña) drives Hadley cell contraction (expansion) due to upper tropospheric heating (cooling) within the tropics, which drives an equatorward (poleward) shift of the subtropical jet stream (Robinson, 2002; Lu et al., 2008). Given the known interannual variability of the Hadley circulation, recent studies have focused on the degree to which similar modulations occur on multidecadal timescales. Specifically, targeted modeling experiments have shown that low-frequency tropical Pacific forcing associated with the observed shift from a positive to a negative PDV phase can account for much of the observed trend since 1980, particularly in the NH (Allen et al., 2014; Allen and Kovilakam, 2017; Amaya et al., 2018).

The PDV-driven multidecadal modulations of the Hadley circulation have important implications for interpreting future climate change projections. To illustrate this concept, we utilize simulations from the Max Planck Institute Grand Ensemble (MPI-GE; Maher et al., 2019). The MPI-GE features a 100-member ensemble of coupled climate model simulations, each forced with the same historical radiative forcings from 1850 to 2005. We further extend our analysis beyond 2005 with model data forced with the RCP8.5 emissions pathway. Since each member is initialized with a slightly different initial condition, internal climate variations are incoherent across the ensemble. Therefore, the MPI-GE ensemble spread provides the opportunity to investigate the influence of low-frequency coupled climate modes in relation to the externally forced signal common to each member.

A common metric used to measure the Hadley cell edge is the latitude at which the meridional overturning streamfunction (ψ) at 500mb is equal to zero polewards of the ITCZ ($\psi_{500} = 0$). This metric is part of a class of lower tropospheric Hadley cell edge indicators that strongly co-vary with each other from year-to-year and show a direct linkage to surface impacts (Davis and Birner, 2017; Staten et al., 2018). The streamfunction can be calculated as:

$$\psi(P,\phi) = \frac{2a\cos\phi}{g}\int_0^P [v]dp \tag{3}$$

where a is the radius of the Earth, g is gravitational acceleration, ϕ is latitude, P is some arbitrary pressure level, and v is the meridional wind component, with brackets denoting the zonal average. For each MPI-GE member, we use annual mean ψ to calculate the $\psi_{500} = 0$ trend (°latitude decade^{-1}) in each hemisphere over the 30-year period 1985–2014 using a linear least-squares fit. We then calculate SSTA* trends (°C decade^{-1}) over the same time period for each member and at each grid point, where the superscript * represents deviations from the ensemble mean. A careful comparison of these two variables allows us to investigate which (if any) internal SSTA patterns can explain the spread in the model's estimate of forced Hadley cell expansion from 1985 to

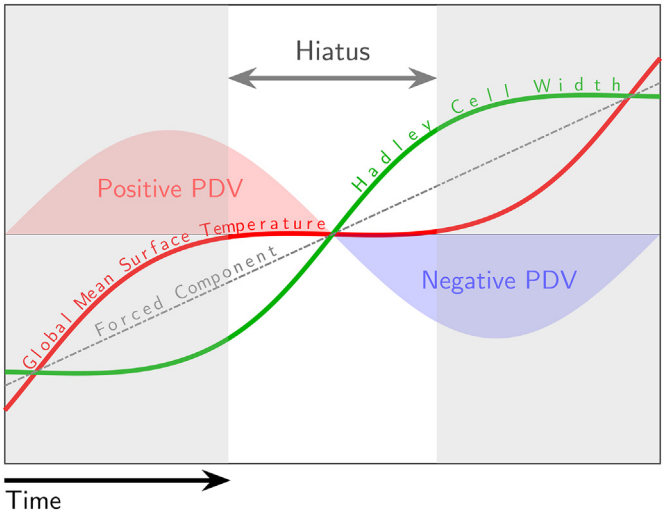

Fig. 10. Schematic illustration demonstrating the influence of PDV (red/blue shading) on Global Mean Surface Temperature (GMST; red line) and Hadley cell width (green line). During the multidecadal transition from a positive PDV phase to negative PDV phase, the long-term rise in GMST due to anthropogenic forcing (grey line) is partially compensated by internal cooling, resulting in a warming slowdown. In contrast, the superposition of internal and forced trends leads to a concurrent accelerated Hadley cell expansion. This thought experiment can be applied to other combinations of internal decadal climate variability and climate change metrics discussed in the text. Figure adapted from Amaya et al. (2018).

2014.

Fig. 9a shows the correlation of the ensemble spread of total (NH + SH) $\psi_{500} = 0$ trends with the ensemble spread of SSTA* trends at each grid point. Consistent with previous studies, the correlation map reveals a negative PDV-like pattern (cf. Fig. 1a), suggesting that multidecadal trends in tropical Pacific climate variability can significantly modulate the model's representation of the forced Hadley cell edge trend (Allen and Kovilakam, 2017; Amaya et al., 2018). This relationship is readily apparent in Fig. 9b, which compares each ensemble member's total $\psi_{500} = 0$ trend with its SSTA* trends averaged in the Niño3.4 region (5°S - 5°N, 120°W - 170°W) (i.e., Niño3.4*). Within the MPI-GE, Hadley cell edge trends and Niño3.4* trends are significantly anti-correlated at $R = -0.63$. This suggests that ensemble members experiencing a decadal cooling in the tropical Pacific from 1985 to 2014 tend to have accelerated Hadley cell expansion relative to the ensemble mean or forced expansion (horizontal black line). This relationship is summarized in the schematic illustration depicted in Fig. 10. Note that this thought experiment can be applied to other forms of decadal climate variability and other climate change metrics discussed in this review.

The opposite is true of ensemble members with warming trends in the tropical Pacific, which tend to have Hadley cells that are either expanding slower than the ensemble mean or even contracting. The presence of contracting trends in the MPI-GE highlights the dominance of internal noise over the relatively weak (~0.15° latitude decade^{-1}) forced signal in recent decades (Amaya et al., 2018; Quan et al., 2018). Further, estimates of this observed Niño3.4 cooling (horizontal whiskers) fall well within the spread of MPI-GE generated Niño3.4* trends, supporting research that suggests the recent PDV phase transition can be explained by internal climate variations alone (Newman et al., 2016).

Moving forward there are myriad outstanding research questions that must be addressed in order to improve predictability of future Hadley cell width changes. First, although ENSO- and PDV-driven Hadley cell width variations represent the dominant form of internal variations (Amaya et al., 2018), they are not the only climate modes that influence the edge of subtropical dry zones. For example, recent multidecadal trends of the Northern and Southern Annular Modes to more positive phases may have contributed to recent Hadley cell expansion as well (e.g., Previdi and Liepert, 2007). Further, the North Atlantic Oscillation and AMV have also been linked to Hadley Cell width variability in the NH (Lucas and Nguyen, 2015).

Second, recent literature has highlighted the importance of maintaining a regional perspective when investigating Hadley cell width variations. Zonal mean Hadley cell metrics are useful tools that simplify otherwise complicated dynamics; however, such indices limit quantitative analysis on the regional level where impacts are felt. Preliminary studies on this topic show promise in regressing SLP, precipitation, and evaporation onto zonal mean Hadley cell width metrics (e.g., Schmidt and Grise, 2017; Amaya et al., 2018), while others have also made progress by decomposing the meridional streamfunction into regional components using the Helmholtz Decomposition (Staten et al., 2019). Regardless, future work is needed to elucidate the regional manifestation of the zonal mean Hadley cell response to internal and forced variations.

Finally, although internal variability has contributed a large portion of the observed Hadley cell width trend, the anthropogenic signal will become increasingly important as GHGs continue to accumulate in the atmosphere. Current estimates from coupled climate models suggest that forced Hadley cell expansion in the zonal mean SH (NH) will emerge beyond the range of internal variations by the mid- (late-) 21st century (Quan et al., 2018; Grise et al., 2019). However, as stratospheric ozone continues to recover in the SH (e.g., Eyring et al., 2007; Staten et al., 2018) and as the PDV cycle transitions to a warm phase (Fig. 9b), we expect a slowdown in Hadley cell expansion until such time as the forced signal dominates.

8. Summary and discussion

The human influence on the climate is clear (IPCC, 2014), and this influence has manifested through significant trends in many metrics of observed global climate change. Over the past few decades, however, several key metrics of global change experienced notable changes. The GMST increase underwent an apparent slowdown, Antarctic sea ice expanded, boreal summer Arctic sea ice declined rapidly, both cold and warm extreme occurrences increased over NH continents, and the Hadley circulation expanded poleward (Fig. 4). Many of these changes deviated substantially from the expected trends resulting from increasing GHG forcing, calling into question whether these recent changes indicate fundamental deficiencies in our understanding and simulation of radiatively forced changes of these key metrics or if internal climate variability alone is sufficient to explain these deviations. The global warming hiatus from the late 1990s through the early 2010s received particularly wide attention, providing a focus for scientific inquiry into the sources of variability for GMST and other important metrics.

Recent work has significantly advanced our understanding of the multidecadal variability of these key metrics, providing insight into modulations by internal climate variability. These studies expanded our focus beyond the question of whether internal variability *can* explain these deviations from the expected changes, which often reduces the problem to a matter of statistical significance, to the question of *how* internal variability may explain these deviations, through process-oriented studies that have attempted to understand the observed realization of internal variability. This research brought a closer integration of the climate change and climate variability communities, capitalizing on the merging of unique perspectives and traditions.

A common theme emerging from these studies is the prominent role of decadal-to-multidecadal SST variability, as both the PDV and AMV played important roles in multidecadal modulations of GMST, polar temperature and sea ice, continental extreme temperature occurrence, and Hadley circulation expansion/contraction. These modes of

variability have patterns that are unique from the more spatially uniform response to GHG warming, resulting in distinct seasonal and regional climate impacts but projecting onto these metrics of global climate change. Because of these multidecadal modulations, the trends of these metrics must be calculated over several decades to suppress the noise of internal variability. The hiatus demonstrated that GMST internal variability can overcome the effects of radiative forcing over periods of about 15 years. For other more regionally confined metrics, this timescale tends to be even longer and may extend beyond available observational records; for example, the forced changes in Hadley circulation expansion may not begin to emerge from the noise of internal variability until the mid-21st century (cf. Section 7).

Despite the rapid research progress over the past decade, several challenges remain, particularly with respect to the brevity of the observational record and the limitations of CGCMs in simulating internal, multidecadal climate variability and potentially radiatively forced changes that project onto these modes of variability. The period over which we have reliable observations is relatively short, limiting the number of independent realizations of observed multidecadal variability. Uncertainties in many observational datasets, such as sea ice, increase substantially or become entirely unavailable before the beginning of the satellite era in the late 1970s. Other datasets with records extending more than a century, such as global SST, still have large uncertainties in the first half of the 20th century (Kent et al., 2017), particularly over the Southern Ocean due to limited observations. Because of these uncertainties, many existing SST reconstructions may have underestimated the amplitude of early 20th century AMV and PDV, hindering our ability to understand concomitant climate changes such as accelerated Arctic warming (Tokinaga et al., 2017). Reconstructions through paleoclimate proxies have yielded PDV (e.g., Henley, 2017) and AMV (e.g., Zhang et al., 2019c) records extending back hundreds of years, and sometimes longer, but these reconstructions expectedly have higher uncertainty than the instrumental records. Nevertheless, efforts to improve the length and reliability of the observed record for these modes of internal variability and the metrics they affect remain a worthwhile endeavor.

In addition, available evidence suggests that although state-of-the-art CGCMs simulate the basic structure of the dominant decadal modes of variability, they generally underestimate the amplitude of some important modes of internal multidecadal variability. As discussed in Section 2, climate models generally underestimate both PDV and AMV. The decadal-to-multidecadal component of the North Atlantic Oscillation is also underestimated in CMIP5 models (Wang et al., 2017b), which has important consequences for the simulation of Northern Hemisphere mean (Wang et al., 2017b) and extreme (Johnson et al., 2018) temperature occurrence. Such biases likely relate to deficiencies in simulating slow ocean processes, such as the AMOC (Wang et al., 2017b; Kim et al., 2018a; Yan et al., 2018), and coupled ocean-atmosphere interactions (e.g., Bellomo et al., 2016). Large spreads exist among models in tropical Pacific SST variance and its impact on GMST (Wang et al., 2017a), although the cause is unclear. This underestimation of internal multidecadal variability makes it challenging to disentangle errors in radiatively forced trends versus errors in simulated internal variability when assessing significant trend differences between climate models and observations.

The aforementioned challenges call for sustained efforts in improving paleoclimate and long-term observations while also addressing model biases through a hierarchy of modeling approaches. Despite these current limitations in both observations and CGCMs, the community has employed and should continue to pursue innovative hybrid approaches that combine observational analysis with state-of-the-art climate modeling to disentangle the effects of internal climate variability from radiatively forced changes. The key element of this pursuit is the ability to distinguish distinct spatial and/or temporal fingerprints between internal variability, which tends to be spatially heterogeneous, and GHG forced changes, which tend to be more spatially uniform, and then to use the evolution of observed fingerprints as a constraint.

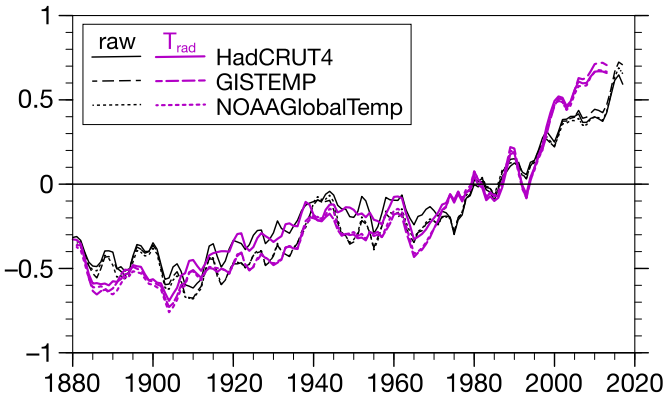

Fig. 11. Estimating the radiatively forced GMST changes through a hybrid observational/climate modeling approach. Three-year running mean GMST anomalies (K) relative to 1970–1999 average. Raw anomalies (black) and radiatively-forced anomalies estimated following Kosaka and Xie, 2016 (purple). Based on HadCRUT4.6.0.0, GISTEMP v4, NOAAGlobalTemp version 5, and CM2.1 historical-RCP4.5 and pacemaker simulations as used in Fig. 2.

An application of the tropical pacemaker experiments described in Section 3 represents one such approach. Given the success of the pacemaker experiment in simulating the observed GMST time series, and that the multidecadal variability of observed tropical Pacific SST is expected to be dominated by internal variability, Kosaka and Xie, 2016 inferred the radiatively forced GMST response as $T_{rad} = T_{obs} - (T_{PM} - T_{HIST})$, where T_{obs} is the observed GMST time series and the term in parenthesis (ensemble mean GMST difference between the tropical Pacific pacemaker and historical simulations) represents internal variability induced by tropical Pacific SST. The time series of T_{rad} shows a steeper climb from about 1900 through the early 2010s when the hiatus ended (Fig. 11), indicating that the centennial trend in observed GMST may have underestimated the true radiatively forced trend owing to the effects of internal variability, at least until the sharp rise in GMST following the end of the hiatus in 2014 (Hu and Fedorov, 2017; Su et al., 2017). The method of Kosaka and Xie et al. (2016) represents one approach to estimating the influence of PDV on GMST that may be complemented by other approaches that use more direct estimates of PDV-related GMST changes from long unforced climate model control runs (Meehl et al., 2016b).

The growing availability of large ensembles from several CGCMs, where external forcing is held the same but initial conditions are varied, also has benefited the study of internal multidecadal climate variability. For example, Ding et al. (2019) analyzed simulations of the Community Earth System Model Large Ensemble (Kay et al., 2015) to determine the role of internal multidecadal variability on the observed September Arctic sea ice trend. Because the simulations reveal that the forced and internal fingerprints of Arctic circulation change are quite distinct, they were able to apply a pattern-matching technique to decompose the observed Arctic circulation and related sea ice trends into radiatively forced and internal components (Fig. 6). Therefore, the analysis relied on the CGCM to simulate realistic patterns of forced and internal climate variability but also relied on the observed variability to constrain the temporal evolution of the two components. In general, the increasing availability of CGCM large ensembles has enhanced our ability to test methods of distinguishing internal variability from radiatively forced changes in a single realization of nature, which include methods to separate the influence of external radiative forcing on the AMV and PDV (Si and Hu, 2017; Xu and Hu, 2018).

Other recent approaches have applied novel statistical approaches to observational data alone in order to distinguish radiatively forced changes from internal variability and to diagnose CGCM errors. The method of “dynamical adjustment” (Smoliak et al., 2010; Wallace et al.,

2012) was introduced as a means of decomposing observed climate trends into dynamic and thermodynamic components by statistically separating the component of the trend related to atmospheric circulation (dynamic component) from the residual component attributed to thermodynamic processes. If the radiatively forced circulation trends are expected to be much weaker than the internal component, such as in wintertime extratropical circulation trends, then the dynamic component is primarily attributed to internal climate variability, and the thermodynamic component is primarily attributed to radiative forcing. Another recent observations-based approach relies on statistical resampling of historical data to construct "observational large ensembles" (McKinnon et al., 2017); comparisons of internal variability in observational large ensembles with that of CGCMs may provide insights into CGCM internal variability amplitude biases.

The recent developments of these approaches signify potential advances in compensating for CGCM deficiencies and in disentangling internal multidecadal variability from radiatively forced changes for many key metrics of global climate change. Importantly, these methodologies point toward pathways for near real-time diagnoses of the effects of internal variability so that we may identify the sources of modulation of these metrics as it occurs, informing on how these sources either constructively or destructively interfere with the radiatively forced trend. As with the recent hiatus, it is inevitable that destructive interference by the effects of these internal modes will offset and possibly even temporarily reverse the radiatively forced trends for each of these metrics over decadal to multidecadal periods. The insights gained through the past decade of research have better prepared the community to address these modulations as they occur.

Declaration of Competing Interest

The authors declare that they have no known competing financial interests or personal relationships that could have appeared to influence the work reported in this paper.

Acknowledgments

We thank Drs. Liwei Jia and Hiroyuki Murakami for helpful comments on an earlier version of the manuscript as well as Dr. Aixue Hu and an anonymous reviewer for constructive comments that improved this manuscript. N.C.J. is supported by award NA18OAR4320123 from the NOAA, U.S. Department of Commerce. D.J.A. and S.-P.X. are supported by the National Science Foundation (AGS -1637450). Q.-H. D. is supported by NSF's Polar Programs (OPP-1744598) and NOAA's Climate Program Office (NA18OAR4310424 and NA19OAR4310281). Y.K. is supported by the Japan Ministry of Education, Culture, Sports, Science and Technology through the Integrated Research Program for Advancing Climate Models and the Arctic Challenge for Sustainability project, by the Japan Science and Technology Agency through Belmont Forum CRA "InterDec", and by Japan Society for the Promotion of Science (JSPS) KAKENHI Grants 18H01278, 19H01964, and 19H05703. H.T. is supported by JSPS KAKENHI Grants 18H03726 and 19H05704. H.T. and Y.K. are also supported by JSPS KAKENHI 18H01281. Shang-Min Long of Hohai University provided Fig. 5.

References

Alexander, M.A., Bhatt, U.S., Walsh, J.E., Timlin, M.S., Miller, J.S., Scott, J.D., 2004. The atmospheric response to realistic Arctic Sea ice anomalies in an AGCM during winter. J. Clim. 17, 890–905. https://doi.org/10.1175/1520-0442(2004)017<0890:TARTRA>2.0.CO;2.

Alexeev, V.A., Langen, P.L., Bates, J.R., 2005. Polar amplification of surface warming on an aquaplanet in "ghost forcing" experiments without sea ice feedbacks. Clim. Dyn. 24, 655–666. https://doi.org/10.1007/s00382-005-0018-3.

Allen, R.J., Kovilakam, M., 2017. The role of natural climate variability in recent tropical expansion. J. Clim. https://doi.org/10.1175/JCLI-D-16-0735.1. JCLI-D-16-0735.1.

Allen, R.J., Sherwood, S.C., Norris, J.R., Zender, C.S., 2012. Recent Northern Hemisphere tropical expansion primarily driven by black carbon and tropospheric ozone. Nature 485, 350–354. https://doi.org/10.1038/nature11097.

Allen, R.J., Norris, J.R., Kovilakam, M., 2014. Influence of anthropogenic aerosols and the Pacific Decadal Oscillation on tropical belt width. Nat. Geosci. 7, 270–274. https://doi.org/10.1038/ngeo2091.

Amaya, D.J., 2019. The Pacific Meridional Mode and ENSO: a Review. Curr. Clim. Chang. Reports. https://doi.org/10.1007/s40641-019-00142-x.

Amaya, D.J., Xie, S.P., Miller, A.J., McPhaden, M.J., 2015. Seasonality of tropical Pacific decadal trends associated with the 21st century global warming hiatus. J. Geophys. Res. Ocean. 120, 6782–6798. https://doi.org/10.1002/2015JC010906.

Amaya, D.J., DeFlorio, M.J., Miller, A.J., Xie, S.P., 2017. WES feedback and the Atlantic Meridional Mode: observations and CMIP5 comparisons. Clim. Dyn. 49, 1665–1679. https://doi.org/10.1007/s00382-016-3411-1.

Amaya, D.J., Siler, N., Xie, S.P., Miller, A.J., 2018. The interplay of internal and forced modes of Hadley Cell expansion: lessons from the global warming hiatus. Clim. Dyn. 51, 305–319. https://doi.org/10.1007/s00382-017-3921-5.

Andrews, T., Webb, M.J., 2018. The dependence of global cloud and lapse rate feedbacks on the spatial structure of tropical pacific warming. J. Clim. 31, 641–654. https://doi.org/10.1175/JCLI-D-17-0087.1.

Armour, K., Bitz, C.M., 2015. Observed and Projected Trends in Antarctic Sea Ice. (US Clivar Variations Newsletter).

Armour, K.C., Marshall, J., Scott, J., Donohoe, A., Newsom, E.R., 2016. Southern Ocean warming delayed by circumpolar upwelling and equatorward transport. Nat. Geosci. 9, 549–554. https://doi.org/10.1038/ngeo2731.

Barnes, E.A., Screen, J.A., 2015. The impact of Arctic warming on the midlatitude jetstream: can it? Has it? Will it? WIREs Clim. Change 6, 277–286. https://doi.org/10.1002/wcc.337.

Baxter, I., Ding, Q.D., Schweiger, A., L'Heureux, M., Baxter, S., Wang, T., Zhang, Q., Harnos, K., Markle, B., Topal, D., Lu, J., 2019. How tropical SST changes contributed to accelerated sea ice melt from 2007 to 2012 as ice is thinned by anthropogenic forcing. J. Clim. https://doi.org/10.1175/JCLI-D-18-0783.1. in press.

Bellomo, K., Clement, A.C., Murphy, L.N., Polvani, L.M., Cane, M.A., 2016. New observational evidence for a positive cloud feedback that amplifies the Atlantic Multidecadal Oscillation. Geophys. Res. Lett. 43, 9852–9859. https://doi.org/10.1002/2016GL069961.

Bengtsson, L., Semenov, V.A., Johannessen, O.M., 2004. The early twentieth-century warming in the Arctic - a possible mechanism. J. Clim. 17, 4045–4057. https://doi.org/10.1175/1520-0442(2004)017%3C4045:TETWIT%3E2.0.CO;2.

Bindoff, N.L., et al., 2013. Detection and Attribution of Climate Change: from Global to Regional. In: Stocker, T.F., Qin, D., Plattner, G.-K., Tignor, M., Allen, S.K., Boschung, J. ... Midgley, P.M. (Eds.), Climate Change 2013: The Physical Science Basis. Contribution of Working Group I to the Fifth Assessment Report of the Intergovernmental Panel on Climate Change. Cambridge University Press, Cambridge, United Kingdom and New York, NY, USA.

Bintanja, R., Graversen, R., Hazeleger, W., 2011. Arctic winter warming amplified by the thermal inversion and consequent low infrared cooling to space. Nat. Geosci. 4, 758–761. https://doi.org/10.1038/ngeo1285.

Bitz, C.M., Polvani, L.M., 2012. Antarctic climate response to stratospheric ozone depletion in a fine resolution ocean climate model. Geophys. Res. Lett. 39https://doi.org/10.1029/2012GL053393. L20705.

Blackport, R., Screen, J.A., van der Wiel, K., Bintanja, R., 2019. Minimal influence of reduced Arctic Sea ice on coincident cold winters in mid-latitudes. Nat. Clim. Chang. 9, 697–704. https://doi.org/10.1038/s41558-019-0551-4.

Bony, S., Colman, R., Kattsov, V.M., Allan, R.P., Bretherton, C.S., Dufresne, J.L., Hall, A., Hallegatte, S., Holland, M.M., Ingram, W., Randall, D.A., Soden, B.J., Tselioudis, G., Webb, M.J., 2006. How well do we understand and evaluate climate change feedback processes? J. Clim. https://doi.org/10.1175/JCLI3819.1.

Boo, K.-O., et al., 2015. Influence of aerosols in multidecadal SST variability simulations over the North Pacific. J. Geophys. Res. Atmos. 120, 517–531. https://doi.org/10.1002/2014JD021933.

Booth, B.B.B., Dunstone, N.J., Halloran, P.R., Andrews, T., Bellouin, N., 2012. Aerosols implicated as a prime driver of twentieth-century North Atlantic climate variability. Nature 484, 228–232. https://doi.org/10.1038/nature10946.

Brönnimann, S., 2009. Early twentieth-century warming. Nat. Geosci. 2, 735–736. https://doi.org/10.1038/ngeo670.

Brown, P.T., Lozier, M.S., Zhang, R., Li, W., 2016. The necessity of cloud feedback for a basin-scale Atlantic Multidecadal Oscillation. Geophys. Res. Lett. 43, 3955–3963. https://doi.org/10.1002/2016GL068303.

Cai, W., Borlace, S., Lengaigne, M., van Rensch, P., Collins, M., Vecchi, G.A., Timmermann, A., Santoso, A., McPhaden, M.J., Wu, L., England, M.H., Wang, G., Guilyardi, E., Jin, F.-F., 2014. Increasing frequency of extreme El Niño events due to greenhouse warming. Nat. Clim. Chang. 4, 111–116. https://doi.org/10.1038/nclimate2100.

Chen, X., Wallace, J.M., 2015. ENSO-like variability: 1900-2013. J. Clim. 28, 9623–9641. https://doi.org/10.1175/JCLI-D-15-0322.1.

Chikamoto, Y., Timmermann, A., Luo, J.-J., Mochizuki, T., Kimoto, M., Watanabe, M., Ishii, M., Xie, S.-P., Jin, F.-F., 2015. Skilful multi-year predictions of tropical trans-basin climate variability. Nat. Commun. 6, 6869. https://doi.org/10.1038/ncomms7869.

Chikamoto, Y., Mochizuki, T., Timmermann, A., Kimoto, M., Watanabe, M., 2016. Potential tropical Atlantic impacts on Pacific decadal climate trends. Geophys. Res. Lett. 43, 7143–7151. https://doi.org/10.1002/2016GL069544.

Choi, Y.-S., Kim, B.-M., Hur, S.-K., Kim, S.-J., Kim, J.-H., Ho, C.-H., 2014. Connecting early summer cloud-controlled sunlight and late summer sea ice in the Arctic. J. Geophys. Res. Atmos. 119. https://doi.org/10.1002/2014JD022013.

Chylek, P., Folland, C.K., Lesins, G., Dubey, M.K., Wang, M.-Y., 2009. Arctic air temperature change amplification and the Atlantic multidecadal oscillation. Geophys.

Res. Lett. 36https://doi.org/10.1029/2009GL038777. L14801.
Clement, A., Bellomo, K., Murphy, L.N., Cane, M.A., Mauritsen, T., Rädel, G., Stevens, B., 2015. The Atlantic multidecadal oscillation without a role for ocean circulation. Science (80-.) 350, 320–324. https://doi.org/10.1126/science.aab3980.
Clement, A., Cane, M.A., Murphy, L.N., Bellomo, K., Mauritsen, T., Stevens, B., 2016. Response to comment on "the Atlantic Multidecadal Oscillation without a role for ocean circulation.". Science 352, 1527. https://doi.org/10.1126/science.aaf2575.
Cohen, J.L., Furtado, J.C., Barlow, M., Alexeev, V.A., Cherry, J.E., 2012. Asymmetric seasonal temperature trends. Geophys. Res. Lett. 39. https://doi.org/10.1029/2011GL050582.
Cohen, J., Screen, J.A., Furtado, J.C., Barlow, M., Whittleston, D., Coumou, D., Francis, J., Dethloff, K., Entekhabi, D., Overland, J., Jones, J., 2014. Recent Arctic amplification and extreme mid-latitude weather. Nat. Geosci. 7, 627–637. https://doi.org/10.1038/ngeo2234.
Cohen, J., Zhang, X., Francis, J., et al., 2020. Divergent consensuses on Arctic amplification influence on midlatitude severe winter weather. Nat. Clim. Chang. 10, 20–29. https://doi.org/10.1038/s41558-019-0662-y.
Colman, R.A., Power, S.B., 2010. Atmospheric radiative feedbacks associated with transient climate change and climate variability. Clim. Dyn. 34, 919–933. https://doi.org/10.1007/s00382-009-0541-8.
Compo, G.P., Whitaker, J.S., Sardeshmukh, P.D., Matsui, N., Allan, R.J., Yin, X., Gleason, B.E., Vose, R.S., Rutledge, G., Bessemoulin, P., BroNnimann, S., Brunet, M., Crouthamel, R.I., Grant, A.N., Groisman, P.Y., Jones, P.D., Kruk, M.C., Kruger, A.C., Marshall, G.J., Maugeri, M., Mok, H.Y., Nordli, O., Ross, T.F., Trigo, R.M., Wang, X.L., Woodruff, S.D., Worley, S.J., 2011. The twentieth century reanalysis PROJECT. Q. J. R. Meteorol. Soc. 137, 1–28. https://doi.org/10.1002/qj.776.
Coumou, D., Rahmstorf, S., 2012. A decade of weather extremes. Nat. Clim. Chang. https://doi.org/10.1038/nclimate1452.
Cowtan, K., Way, R.G., 2014. Coverage bias in the HadCRUT4 temperature series and its impact on recent temperature trends. Q. J. R. Meteorol. Soc. 140, 1935–1944. https://doi.org/10.1002/qj.2297.
Dai, A., Fyfe, J.C., Xie, S.-P., Dai, X., 2015. Decadal modulation of global surface temperature by internal climate variability. Nat. Clim. Chang. 5, 555–559. https://doi.org/10.1038/nclimate2605.
Dalton, M.M., Shell, K.M., 2013. Comparison of short-term and long-term radiative feedbacks and variability in twentieth-century global climate model simulations. J. Clim. 26, 10051–10070. https://doi.org/10.1175/JCLI-D-12-00564.1.
Davis, N., Birner, T., 2017. On the discrepancies in tropical belt expansion between reanalyses and climate models and among tropical belt width metrics. J. Clim. 30, 1211–1231. https://doi.org/10.1175/JCLI-D-16-0371.1.
Dee, D.P., Uppala, S.M., Simmons, A.J., Berrisford, P., Poli, P., Kobayashi, S., Andrae, U., Balmaseda, M.A., Balsamo, G., Bauer, P., Bechtold, P., Beljaars, A.C.M., van de Berg, L., Bidlot, J., Bormann, N., Delsol, C., Dragani, R., Fuentes, M., Geer, A.J., Haimberger, L., Healy, S.B., Hersbach, H., Hólm, E.V., Isaksen, L., Kållberg, P., Köhler, M., Matricardi, M., Mcnally, A.P., Monge-Sanz, B.M., Morcrette, J.J., Park, B.K., Peubey, C., de Rosnay, P., Tavolato, C., Thépaut, J.N., Vitart, F., 2011. The ERA-Interim reanalysis: Configuration and performance of the data assimilation system. Q. J. R. Meteorol. Soc. 137, 553–597. https://doi.org/10.1002/qj.828.
Delsole, T., Tippett, M.K., Shukla, J., 2011. A significant component of unforced multidecadal variability in the recent acceleration of global warming. J. Clim. 24, 909–926. https://doi.org/10.1175/2010JCLI3659.1.
Deser, C., Sun, L., Tomas, R.A., Screen, J., 2016. Does ocean coupling matter for the northern extratropical response to projected Arctic Sea ice loss? Geophys. Res. Lett. 43, 2149–2157. https://doi.org/10.1002/2016GL067792.
Deser, C., Guo, R., Lehner, F., 2017. The relative contributions of tropical Pacific Sea surface temperatures and atmospheric internal variability to the recent global warming hiatus. Geophys. Res. Lett. 44, 7945–7954. https://doi.org/10.1002/2017GL074273.
Dessler, A.E., 2013. Observations of climate feedbacks over 2000-10 and comparisons to climate models. J. Clim. 26, 333–342. https://doi.org/10.1175/JCLI-D-11-00640.1.
Ding, Q., Steig, E.J., 2013. Temperature change on the Antarctic Peninsula linked to the tropical Pacific. J. Clim. 26, 7570–7585. https://doi.org/10.1175/JCLI-D-12-00729.1.
Ding, Q., Steig, E.J., Battisti, D.S., Küettel, M., 2011. Winter warming in West Antarctica caused by central tropical Pacific warming. Nat. Geosci. 4, 398–403. https://doi.org/10.1038/ngeo1129.
Ding, Q., Steig, E.J., Battisti, D.S., Wallace, J.M., 2012. Influence of the tropics on the Southern Annular Mode. J. Clim. 25, 6330–6363. https://doi.org/10.1175/JCLI-D-11-00523.1.
Ding, Q.H., Wallace, J.M., Battisti, D.S., Steig, E.J., Gallant, A.J.E., Kim, H.J., Geng, L., 2014. Tropical forcing of the recent rapid Arctic warming in northeastern Canada and Greenland. Nature 509, 209–212. https://doi.org/10.1038/nature13260.
Ding, Q.H., Schweiger, A., L'Heureux, M., Battisti, D.S., Po-Chedley, S., Johnson, N.C., Blanchard-Wrigglesworth, E., Harnos, K., Zhang, Q., Eastman, R., Steig, E.J., 2017. Influence of the recent high-latitude atmospheric circulation change on summertime Arctic Sea ice. Nat. Clim. Chang. 7, 289–295. https://doi.org/10.1038/nclimate3241.
Ding, Q., et al., 2019. Fingerprints of internal drivers of Arctic Sea ice loss in observations and model simulations. Nat. Geosci. 12, 28–33. https://doi.org/10.1038/s41561-018-0256-8.
Donat, M.G., Alexander, L.V., Yang, H., Durre, I., Vose, R., Dunn, R.J.H., Willett, K.M., Aguilar, E., Brunet, M., Caesar, J., Hewitson, B., Jack, C., Klein Tank, A.M.G., Kruger, A.C., Marengo, J., Peterson, T.C., Renom, M., Oria Rojas, C., Rusticucci, M., Salinger, J., Elrayah, A.S., Sekele, S.S., Srivastava, A.K., Trewin, B., Villarroel, C., Vincent, L.A., Zhai, P., Zhang, X., Kitching, S., 2013. Updated analyses of temperature and precipitation extreme indices since the beginning of the twentieth century: the HadEX2 dataset. J. Geophys. Res. Atmos. 118, 2098–2118. https://doi.org/10.1002/jgrd.50150.
Dong, L., McPhaden, M.J., 2017. Why has the relationship between Indian and Pacific Ocean decadal variability changed in recent decades? J. Clim. 30, 1971–1983. https://doi.org/10.1175/JCLI-D-16-0313.1.
Dong, L., Zhou, T., Chen, X., 2014. Changes of Pacific decadal variability in the twentieth century driven by internal variability, greenhouse gases, and aerosols. Geophys. Res. Lett. 41, 8570–8577. https://doi.org/10.1002/2014GL062269.
d'Orgeville, M., Peltier, W.R., 2007. On the Pacific Decadal Oscillation and the Atlantic Multidecadal Oscillation: Might they be related? Geophys. Res. Lett. 34https://doi.org/10.1029/2007GL031584. n/a-n/a.
Easterling, D.R., Wehner, M.F., 2009. Is the climate warming or cooling? Geophys. Res. Lett. 36https://doi.org/10.1029/2009GL037810. L08706.
England, M.H., McGregor, S., Spence, P., Meehl, G.A., Timmermann, A., Cai, W., Gupta, A. Sen, McPhaden, M.J., Purich, A., Santoso, A., 2014. Recent intensification of wind-driven circulation in the Pacific and the ongoing warming hiatus. Nat. Clim. Chang. 4, 222–227. https://doi.org/10.1038/nclimate2106.
Eyring, V., Waugh, D.W., Bodeker, G.E., Cordero, E., Akiyoshi, H., Austin, J., Beagley, S.R., Boville, B.A., Braesicke, P., Brühl, C., Butchart, N., Chipperfield, M.P., Dameris, M., Deckert, R., Deushi, M., Frith, S.M., Garcia, R.R., Gettelman, A., Giorgetta, M.A., Kinnison, D.E., Mancini, E., Manzini, E., Marsh, D.R., Matthes, S., Nagashima, T., Newman, P.A., Nielsen, J.E., Pawson, S., Pitari, G., Plummer, D.A., Rozanov, E., Schraner, M., Scinocca, J.F., Semeniuk, K., Shepherd, T.G., Shibata, K., Steil, B., Stolarski, R.S., Tian, W., Yoshiki, M., 2007. Multimodel projections of stratospheric ozone in the 21st century. J. Geophys. Res. Atmos. 112. https://doi.org/10.1029/2006JD008332.
Fan, T., Deser, C., Schneider, D.P., 2014. Recent Antarctic Sea ice trends in the context of Southern Ocean surface climate variations since 1950. Geophys. Res. Lett. 41, 2419–2426. https://doi.org/10.1002/2014GL059239.
Fang, C., Wu, L., Zhang, X., 2014. The impact of global warming on the Pacific Decadal Oscillation and the possible mechanism. Adv. Atmos. Sci. 31, 118–130. https://doi.org/10.1007/s00376-013-2260-7.
Farneti, R., Molteni, F., Kucharski, F., 2014. Pacific interdecadal variability driven by tropical-extratropical interactions. Clim. Dyn. 42, 3337–3355. https://doi.org/10.1007/s00382-013-1906-6.
Fogt, R.L., Perlwitz, L., Monaghan, A.J., Bromwich, D.H., Jones, J.M., Marshall, G.J., 2009. Historical SAM variability. Part II. Twentieth-Century variability and trends from reconstructions, observations, and the IPCC AR4 Model. J. Clim. 22, 5346–5365. https://doi.org/10.1175/2009JCLI2786.1.
Folland, C.K., Palmer, T.N., Parker, D.E., 1986. Sahel rainfall and worldwide sea temperatures, 1901-85. Nature 320, 602–607. https://doi.org/10.1038/320602a0.
Forster, P.M.D.F., Gregory, J.M., 2006. The climate sensitivity and its components diagnosed from earth radiation budget data. J. Clim. 19, 39–52. https://doi.org/10.1175/JCLI3611.1.
Foster, G., Rahmstorf, S., 2011. Global temperature evolution 1979–2010. Environ. Res. Lett. 6https://doi.org/10.1088/1748-9326/6/4/044022. 044022.
Francis, J.A., Hunter, E., 2006. New insight into the disappearing Arctic Sea ice. Eos Trans. AGU 87, 509–511. https://doi.org/10.1029/2006EO460001.
Francis, J.A., Vavrus, S.J., 2012. Evidence linking Artic amplification to extreme weather in mid-latitudes. Geophys. Res. Lett. 39https://doi.org/10.1029/2012GL051000. L06801.
Fyfe, J.C., von Salzen, K., Gillett, N.P., Arora, V.K., Flato, G.M., McConnell, J.R., 2013. One hundred years of Arctic surface temperature variation due to anthropogenic influence. Sci. Rep. 3, 2645. https://doi.org/10.1038/srep02645.
Fyfe, J.C., Meehl, G.A., England, M.H., Mann, M.E., Santer, B.D., Flato, G.M., Hawkins, E., Gillett, N.P., Xie, S.-P., Kosaka, Y., Swart, N.C., 2016. Making sense of the early-2000s warming slowdown. Nat. Clim. Chang. 6, 224–228. https://doi.org/10.1038/nclimate2938.
Goosse, H., Lefebvre, W., de Montety, A., Crespin, E., Orsi, A., 2009. Consistent past half-century trends in the atmosphere, the sea ice and the ocean at high Southern Latitudes. Clim. Dyn. 33, 999–1016. https://doi.org/10.1007/s00382-008-0500-9.
Grant, A.N., Bronnimann, S., Ewen, T., Griesser, T., Stickler, A., 2009. The early twentieth century warm period in the European Arctic. Meteorol. Z. 18, 425–432. https://doi.org/10.1127/0941-2948/2009/0391.
Graversen, R.G., Wang, M., 2009. Polar amplification in a coupled climate model with locked albedo. Clim. Dyn. 33, 629–643. https://doi.org/10.1007/s00382-009-0535-6.
Graversen, R.G., Mauritsen, T., Tjernstrom, M., Kallen, E., Svensson, G., 2008. Vertical structure of recent Arctic warming. Nature 451, 53–56. https://doi.org/10.1038/nature06502.
Gregory, J.M., Andrews, T., 2016. Variation in climate sensitivity and feedback parameters during the historical period. Geophys. Res. Lett. 43, 3911–3920. https://doi.org/10.1002/2016GL068406.
Gregory, J.M., Ingram, W.J., Palmer, M.A., Jones, G.S., Stott, P.A., Thorpe, R.B., Lowe, J.A., Johns, T.C., Williams, K.D., 2004. A new method for diagnosing radiative forcing and climate sensitivity. Geophys. Res. Lett. 31. https://doi.org/10.1029/2003GL018747.
Grise, K.M., Davis, S.M., Simpson, I.R., Waugh, D.W., Fu, Q., Allen, R.J., Rosenlof, K.H., Ummenhofer, C.C., Karnauskas, K.B., Maycock, A.C., Quan, X.W., Birner, T., Staten, P.W., 2019. Recent tropical expansion: Natural variability or forced response? J. Clim. 32, 1551–1571. https://doi.org/10.1175/JCLI-D-18-0444.1.
Gu, D., Philander, S.G.H., 1997. Interdecadal climate fluctuations that depend on exchanges between the tropics and extratropics. Science 275, 805–807. https://doi.org/10.1126/science.275.5301.805.
Han, W., Meehl, G.A., Hu, A., Alexander, M.A., Yamagata, Y., Yuan, D., Ishii, M., Pegion, P., Zheng, J., Hamlington, B.D., Quan, X.-W., Leben, R.R., 2014. Intensification of decadal and multi-decadal sea level variability in the western tropical Pacific during

recent decades. Clim. Dyn. 43, 1357–1379. https://doi.org/10.1007/s00382-013-1951-1.
Hansen, J., Nazarenko, L., 2004. Soot climate forcing via snow and ice albedo. Proc. Natl. Acad. Sci. 101, 423–428. https://doi.org/10.1073/pnas.2237157100.
Hausfather, Z., Cowtan, K., Clarke, D.C., Jacobs, P., Richardson, M., Rohde, R., 2017. Assessing recent warming using instrumentally homogeneous sea surface temperature records. Sci. Adv. 3https://doi.org/10.1126/sciadv.1601207. e1601207.
Henley, B.J., 2017. Pacific decadal climate variability: Indices, patterns and tropical-extratropical interactions. Glob. Planet. Chang. 155, 42–55. https://doi.org/10.1016/j.gloplacha.2017.06.004.
Henley, B.J., Gergis, J., Karoly, D.J., Power, S., Kennedy, J., Folland, C.K., 2015. A Tripole Index for the Interdecadal Pacific Oscillation. Clim. Dyn. 45, 3077–3090. https://doi.org/10.1007/s00382-015-2525-1.
Henley, B.J., Meehl, G., Power, S.B., Folland, C.K., King, A.D., Brown, J.N., Karoly, D.J., Delage, F., Gallant, A.J.E., Freund, M., Neukom, R., 2017. Spatial and temporal agreement in climate model simulations of the Interdecadal Pacific Oscillation. Environ. Res. Lett. 12https://doi.org/10.1088/1748-9326/aa5cc8. 044011.
Hoerling, M.P., Eischeid, J., Perlwitz, J., Quan, X., Zhang, T., Pegion, P., 2012. On the increased frequency of mediterranean drought. J. Clim. 25, 2146–2161. https://doi.org/10.1175/JCLI-D-11-00296.1.
Honda, M., Inoue, J., Yamane, S., 2009. Influence of low Arctic Sea-ice minima on anomalously cold Eurasian winters. Geophys. Res. Lett. 36https://doi.org/10.1029/2008GL037079. L08707.
Hu, S., Fedorov, A.V., 2017. The extreme El Niño of 2015-2016 and the end of global warming hiatus. Geophys. Res. Lett. 44, 3816–3824. https://doi.org/10.1002/2017GL072908.
Huang, B., Thorne, P.W., Banzon, V.F., Boyer, T., Chepurin, G., Lawrimore, J.H., Menne, M.J., Smith, T.M., Vose, R.S., Zhang, H.M., 2017. Extended reconstructed Sea surface temperature, Version 5 (ERSSTv5): upgrades, validations, and intercomparisons. J. Clim. 30, 8179–8205. https://doi.org/10.1175/JCLI-D-16-0836.1.
Inoue, J., Hori, M.E., Takaya, K., 2012. The role of barents sea ice in the wintertime cyclone track and emergence of a warm-Arctic cold-Siberian anomaly. J. Clim. 25, 2561–2569. https://doi.org/10.1175/JCLI-D-11-00449.1.
IPCC, 2014. Climate change 2014: synthesis report. In: Team, Core Writing, Pachauri, R.K., Meyer, L.A. (Eds.), Contribution of Working Groups I, II and III to the Fifth Assessment Report of the Intergovernmental Panel on Climate Change. IPCC, Geneva, Switzerland, pp. 151.
Johannessen, O.M., et al., 2004. Arctic climate change: observed and modelled temperature and sea-ice variability. Tellus A 56, 328–341. https://doi.org/10.1111/j.1600-0870.2004.00060.x.
Johnson, N.C., Xie, S.P., Kosaka, Y., Li, X., 2018. Increasing occurrence of cold and warm extremes during the recent global warming slowdown. Nat. Commun. 9, 1724. https://doi.org/10.1038/s41467-018-04040-y.
Jones, G.S., Stott, P.A., Christidis, N., 2013. Attribution of observed historical near-surface temperature variations to anthropogenic and natural causes using CMIP5 simulations. J. Geophys. Res. 118, 4001–4024. https://doi.org/10.1002/jgrd.50239.
Kamae, Y., Shiogama, H., Watanabe, M., Kimoto, M., 2014. Attributing the increase in Northern Hemisphere hot summers since the late 20th century. Geophys. Res. Lett. 41, 5192–5199. https://doi.org/10.1002/2014GL061062.
Karl, T.R., Arguez, A., Huang, B., Lawrimore, J.H., McMahon, J.R., Menne, M.J., Peterson, T.C., Vose, R.S., Zhang, H.M., 2015. Possible artifacts of data biases in the recent global surface warming hiatus. Science 348, 1469–1472. https://doi.org/10.1126/science.aaa5632.
Karoly, D.J., 1989. Southern Hemisphere Circulation Features Associated with El Niño-Southern Oscillation events. J. Clim. 2, 1239–1252. https://doi.org/10.1175/1520-0442(1989)002<1239:shcfaw>2.0.co;2.
Kavvada, A., Ruiz-Barradas, A., Nigam, S., 2013. AMO's structure and climate footprint in observations and IPCC AR5 climate simulations. Clim. Dyn. 41, 1345–1364. https://doi.org/10.1007/s00382-013-1712-1.
Kay, J.E., L'Ecuyer, T., Gettelman, A., Stephens, G., O'Dell, C., 2008. The contribution of cloud and radiation anomalies to the 2007 Arctic Sea ice extent minimum. Geophys. Res. Lett. 35https://doi.org/10.1029/2008GL033451. L08503.
Kay, J.E., Holland, M.M., Jahn, A., 2011. Inter-annual to multi-decadal Arctic Sea ice extent trends in a warming world. Geophys. Res. Lett. 38https://doi.org/10.1029/2011GL048008. L15708.
Kay, J.E., et al., 2015. The Community Earth System Model (CESM) Large Ensemble Project: a community resource for studying climate change in the presence of internal climate variability. Bull. Amer. Meteor. Soc. 96, 1333–1349. https://doi.org/10.1175/BAMS-D-13-00255.1.
Kent, E.C., et al., 2017. A call for new approaches to quantifying biases in observations of sea surface temperature. Bull. Amer. Meteor. Soc. 98, 1601–1616. https://doi.org/10.1175/BAMS-D-15-00251.1.
Kerr, R.A., 2000. A North Atlantic climate pacemaker for the centuries. Science 288, 1984–1985. https://doi.org/10.1126/science.288.5473.1984.
Kim, B.M., Son, S.W., Min, S.K., Jeong, J.H., Kim, S.J., Zhang, X., Shim, T., Yoon, J.H., 2014. Weakening of the stratospheric polar vortex by Arctic Sea-ice loss. Nat. Commun. 5, 4646. https://doi.org/10.1038/ncomms5646.
Kim, W.M., Yeager, S., Chang, P., Danabasoglu, G., 2018a. Low-frequency North Atlantic climate variability in the community earth system model large ensemble. J. Clim. 31, 787–813. https://doi.org/10.1175/JCLI-D-17-0193.1.
Kim, W.M., Yeager, S.G., Danabasoglu, G., 2018b. Key Role of Internal Ocean Dynamics in Atlantic Multidecadal Variability during the last half Century. Geophys. Res. Lett. 45, 13,449–13,457. https://doi.org/10.1029/2018GL080474.
Kirkman, C., Bitz, C.M., 2011. The effect of the sea ice freshwater flux on Southern Ocean temperatures in CCSM3: deep ocean warming and delayed surface warming. J. Clim. 24, 2224–2237. https://doi.org/10.1175/2010JCLI3625.1.
Knight, J.R., Folland, C.K., Scaife, A.A., 2006. Climate impacts of the Atlantic multidecadal oscillation. Geophys. Res. Lett. 33, 17706. https://doi.org/10.1029/2006GL026242.
Kociuba, G., Power, S.B., 2015. Inability of CMIP5 models to simulate recent strengthening of the walker circulation: Implications for projections. J. Clim. 28, 20–35. https://doi.org/10.1175/JCLI-D-13-00752.1.
Koenigk, T., Gao, Y., Gastineau, G., Keenlyside, N., Nakamura, T., Ogawa, F., Orsolini, Y., Semenov, V., Suo, L., Tian, T., Wang, T., Wettstein, J.J., Yang, S., 2019. Impact of Arctic Sea ice variations on winter temperature anomalies in northern hemispheric land areas. Clim. Dyn. 52, 3111–3137. https://doi.org/10.1007/s00382-018-4305-1.
Kosaka, Y., Xie, S.-P., 2013. Recent global-warming hiatus tied to equatorial Pacific surface cooling. Nature 501, 403–407. https://doi.org/10.1038/nature12534.
Kosaka, Y., Xie, S.-P., 2016. The tropical Pacific as a key pacemaker of the variable rates of global warming. Nat. Geosci. 9, 669–673. https://doi.org/10.1038/ngeo2770.
Kucharski, F., Ikram, F., Molteni, F., Farneti, R., Kang, I.S., No, H.H., King, M.P., Giuliani, G., Mogensen, K., 2016. Atlantic forcing of Pacific decadal variability. Clim. Dyn. 46, 2337–2351. https://doi.org/10.1007/s00382-015-2705-z.
Kug, J.S., Jeong, J.H., Jang, Y.S., Kim, B.M., Folland, C.K., Min, S.K., Son, S.W., 2015. Two distinct influences of Arctic warming on cold winters over North America and East Asia. Nat. Geosci. 8, 759–762. https://doi.org/10.1038/ngeo2517.
Lapp, S.L., St. Jacques, J.-M., Barrow, E., Sauchyn, D.J., 2012. GCM projections for the Pacific Decadal Oscillation under greenhouse forcing for the 21st century. Int. J. Climatol. 32, 1423–1442. https://doi.org/10.1002/joc.2364.
Lean, J.L., Rind, D.H., 2008. How natural and anthropogenic influences alter global and regional surface temperatures: 1889 to 2006. Geophys. Res. Lett. 35. https://doi.org/10.1029/2008GL034864.
Lee, S., 2012. Testing of the tropically excited Arctic warming (TEAM) mechanism with traditional El Nino and La Nina. J. Clim. 25, 4015–4022. https://doi.org/10.1175/JCLI-D-12-00055.1.
Lee, S., Gong, T.T., Johnson, N.C., Feldstein, S.B., Pollard, D., 2011. On the possible link between tropical convection and the Northern Hemisphere Arctic surface air temperature change between 1958-2001. J. Clim. 24, 4350–4367. https://doi.org/10.1175/2011JCLI4003.1.
Lenssen, N.J.L., Schmidt, G.A., Hansen, J.E., Menne, M.J., Persin, A., Ruedy, R., Zyss, D., 2019. Improvements in the uncertainty model in the Goddard Institute for Space Studies Surface Temperature (GISTEMP) analysis. J. Geophys. Res. Atmos. 124, 6307–6326. https://doi.org/10.1029/2018JD029522.
Levitus, S., Antonov, J.I., Boyer, T.P., Baranova, O.K., Garcia, H.E., Locarnini, R.A., Mishonov, A.V., Reagan, J.R., Seidov, D., Yarosh, E.S., Zweng, M.M., 2012. World Ocean heat content and thermosteric sea level change (0-2000m), 1955-2010. Geophys. Res. Lett. 39https://doi.org/10.1029/2012GL051106. L10603.
Lewandowsky, S., Risbey, J.S., Oreskes, N., 2015. On the definition and identifiability of the alleged "hiatus" in global warming. Sci. Rep. 5, 16784. https://doi.org/10.1038/srep16784.
Li, X., Holland, D.M., Gerber, E.P., Yoo, C., 2014. Impacts of the north and tropical Atlantic Ocean on the Antarctic Peninsula and sea ice. Nature 505, 538–542. https://doi.org/10.1038/nature12945.
Li, C., Stevens, B., Marotzke, J., 2015. Eurasian winter cooling in the warming hiatus of 1998-2012. Geophys. Res. Lett. 42, 8131–8139. https://doi.org/10.1002/2015GL065327.
Li, X., Xie, S.P., Gille, S.T., Yoo, C., 2016. Atlantic-induced pan-tropical climate change over the past three decades. Nat. Clim. Chang. 6, 275–279. https://doi.org/10.1038/nclimate2840.
Liu, Z., Di Lorenzo, E., 2018. Mechanism and predictability of Pacific Decadal Variability. Curr. Clim. Chang. Reports 4, 128–144. https://doi.org/10.1007/s40641-018-0090-5.
Liu, W., Xie, S.P., 2018. An ocean view of the global surface warming hiatus. Oceanography 31, 72–79. https://doi.org/10.5670/oceanog.2018.217.
Loeb, N.G., Lyman, J.M., Johnson, G.C., Allan, R.P., Doelling, D.R., Wong, T., Soden, B.J., Stephens, G.L., 2012. Observed changes in top-of-the-atmosphere radiation and upper-ocean heating consistent within uncertainty. Nat. Geosci. 5, 110–113. https://doi.org/10.1038/ngeo1375.
Long, S., Xie, S.-P., Du, Y., Liu, Q., Zheng, X., Huang, G., Hu, K., Ying, J., 2019. Effects of ocean slow response under low warming targets. J. Clim. 33, 477–496. https://doi.org/10.1175/JCLI-D-19-021.
Lorenz, D.J., 2014. Understanding Midlatitude Jet Variability and Change using Rossby Wave Chromatography: Poleward-Shifted jets in Response to External Forcing. J. Atmos. Sci. 71, 2370–2389. https://doi.org/10.1175/jas-d-13-0200.1.
Lu, J., Chen, G., Frierson, D.M.W., 2008. Response of the zonal mean atmospheric circulation to El Niño versus global warming. J. Clim. 21, 5835–5851. https://doi.org/10.1175/2008JCLI2200.1.
Lucas, C., Nguyen, H., 2015. Regional characteristics of tropical expansion and the role of climate variability. J. Geophys. Res. Atmos. 120, 1–16. https://doi.org/10.1002/2015JD023130.Received.
Luo, J.J., Masson, S., Behera, S., Delecluse, P., Gualdi, S., Navarra, A., Yamagata, T., 2003. South Pacific origin of the decadal ENSO-like variation as simulated by a coupled GCM. Geophys. Res. Lett. 30, 2250. https://doi.org/10.1029/2003GL018649.
Luo, J.J., Sasaki, W., Masumoto, Y., 2012. Indian Ocean warming modulates Pacific climate change. Proc. Natl. Acad. Sci. U. S. A. 109, 18701–18706. https://doi.org/10.1073/pnas.1210239109.
Magnusdottir, G., Deser, C., Saravanan, R., 2004. The effects of North Atlantic SST and sea ice anomalies on the winter circulation in CCM3. Part I: Main features and storm track characteristics of the response. J. Clim. 17, 857–876. https://doi.org/10.1175/1520-0442(2004)017<0857:TEONAS>2.0.CO;2.
Maher, N., Gupta, A. Sen, England, M.H., 2014. Drivers of decadal hiatus periods in the

20th and 21st centuries. Geophys. Res. Lett. 41, 5978–5986. https://doi.org/10.1002/2014GL060527.
Maher, N., McGregor, S., England, M.H., Gupta, A. Sen, 2015. Effects of volcanism on tropical variability. Geophys. Res. Lett. 42, 6024–6033. https://doi.org/10.1002/2015GL064751.
Maher, N., Milinski, S., Suarez-Gutierrez, L., Botzet, M., Dobrynin, M., Kornblueh, L., Kröger, J., Takano, Y., Ghosh, R., Hedemann, C., Li, C., Li, H., Manzini, E., Notz, D., Putrasahan, D., Boysen, L., Claussen, M., Ilyina, T., Olonscheck, D., Raddatz, T., Stevens, B., Marotzke, J., 2019. The Max Planck institute grand ensemble - enabling the exploration of climate system variability. J. Adv. Model. Earth Syst. https://doi.org/10.1029/2019MS001639. 2019MS001639.
Maksym, T., Stammerjohn, S., Ackley, S., Massom, R., 2012. Antarctic sea ice—A polar opposite? Oceanography 25, 140–151. https://doi.org/10.5670/oceanog.2012.88.
Mann, M.E., Emanuel, K.A., 2006. Atlantic Hurricane trends linked to climate change. Eos (Washington. DC). 87, 233–235. https://doi.org/10.1029/2006EO240001.
Mann, M.E., Steinman, B.A., Miller, S.K., 2014. On forced temperature changes, internal variability, and the AMO. Geophys. Res. Lett. 41, 3211–3219. https://doi.org/10.1002/2014GL059233.
Mantua, N.J., Hare, S.R., Zhang, Y., Wallace, J.M., Francis, R.C., 1997. A Pacific Interdecadal climate Oscillation with Impacts on Salmon Production. Bull. Am. Meteorol. Soc. 78, 1069–1079. https://doi.org/10.1175/1520-0477(1997)078<1069:APICOW>2.0.CO;2.
Marshall, J., Armour, K., Scott, J., Kostov, Y., Hausmann, U., Ferreira, D., Shepherd, T., Bitz, C., 2014. The ocean's role in polar climate change: asymmetric Arctic and Antarctic responses to greenhouse gas and ozone forcing. Philos. Trans. R. Soc. A Math. Phys. Eng. Sci. 372, 20130040. https://doi.org/10.1098/rsta.2013.0040.
Marshall, J., Scott, R., Kyle, C.A., Campin, J.M., Maxwell, K., Romanou, A., 2015. The ocean's role in the transient response of climate to abrupt greenhouse gas forcing. Clim. Dyn. 44, 2287–2299. https://doi.org/10.1007/s00382-014-2308-0.
McCusker, K.E., Fyfe, J.C., Sigmond, M., 2016. Twenty-five winters of unexpected Eurasian cooling unlikely due to Arctic Sea-ice loss. Nat. Geosci. 9, 838–842. https://doi.org/10.1038/ngeo2820.
McGregor, S., Timmermann, A., Stuecker, M.F., England, M.H., Merrifield, M., Jin, F.-F., Chikamoto, Y., 2014. Recent Walker circulation strengthening and Pacific cooling amplified by Atlantic warming. Nat. Clim. Chang. 4, 888–892. https://doi.org/10.1038/nclimate2330.
McKinnon, K.A., Poppick, A., Dunn-Sigouin, E., Deser, C., 2017. An "observational large ensemble" to compare observed and modeled temperature trend uncertainty due to internal variability. J. Clim. 30, 7585–7598. https://doi.org/10.1175/JCLI-D-16-0905.1.
Medhaug, I., Stolpe, M.B., Fischer, E.M., Knutti, R., 2017. Reconciling controversies about the "global warming hiatus.". Nature. https://doi.org/10.1038/nature22315.
Meehl, G.A., Teng, H., 2012. Case studies for initialized decadal hindcasts and predictions for the Pacific region. Geophys. Res. Lett. 39https://doi.org/10.1029/2012GL053423. L22705.
Meehl, G.A., Teng, H., 2014. Regional precipitation simulations for the mid-1970s shift and early-2000s hiatus. Geophys. Res. Lett. 41, 7658–7665. https://doi.org/10.1002/2014GL061778.
Meehl, G.A., Hu, A., Santer, B.D., 2009. The mid-1970s climate shift in the Pacific and the relative roles of forced versus inherent decadal variability. J. Clim. 22, 780–792. https://doi.org/10.1175/2008JCLI2552.1.
Meehl, G.A., Arblaster, J.M., Fasullo, J.T., Hu, A., Trenberth, K.E., 2011. Model-based evidence of deep-ocean heat uptake during surface-temperature hiatus periods. Nat. Clim. Chang. 1, 360–364. https://doi.org/10.1038/nclimate1229.
Meehl, G.A., Hu, A., Arblaster, J.M., Fasullo, J., Trenberth, K.E., 2013. Externally forced and internally generated decadal climate variability associated with the Interdecadal Pacific Oscillation. J. Clim. 26, 7298–7310. https://doi.org/10.1175/JCLI-D-12-00548.1.
Meehl, G.A., Teng, H., Arblaster, J.M., 2014. Climate model simulations of the observed early-2000s hiatus of global warming. Nat. Clim. Chang. 4, 898–902. https://doi.org/10.1038/nclimate2357.
Meehl, G.A., Arblaster, J.M., Bitz, C.M., Chung, C.T.Y., Teng, H., 2016a. Antarctic Sea-ice expansion between 2000 and 2014 driven by tropical Pacific decadal climate variability. Nat. Geosci. 9, 590–595. https://doi.org/10.1038/ngeo2751.
Meehl, G.A., Hu, A., Santer, B.D., Xie, S.-P., 2016b. Contribution of the Interdecadal Pacific Oscillation to twentieth-century global surface temperature trends. Nat. Clim. Chang. 6, 1005–1008. https://doi.org/10.1038/NCLIMATE3107.
Meehl, G.A., Hu, A., Teng, H., 2016c. Initialized decadal prediction for transition to positive phase of the Interdecadal Pacific Oscillation. Nat. Commun. 7, 11718. https://doi.org/10.1038/ncomms11718.
Meehl, G.A., Chung, C.T.Y., Arblaster, J.M., Holland, M.M., Bitz, C.M., 2018. Tropical decadal variability and the rate of Arctic Sea ice decrease. Geophys. Res. Lett. 45, 11326–11333. https://doi.org/10.1029/2018GL079989.
Meehl, G.A., Arblaster, J.M., Chung, C.T.Y., Holland, M.M., DuVivier, Thompson L., Yang, D., Bitz, C.M., 2019. Sustained Ocean changes contributed to sudden Antarctic Sea ice retreat in late 2016. Nat. Commun. 10, 14. https://doi.org/10.1038/s41467-018-07865-9.
Middlemas, E.A., Clement, A.C., 2016. Spatial patterns and frequency of unforced decadal-scale changes in global mean surface temperature in climate models. J. Clim. 29, 6245–6257. https://doi.org/10.1175/JCLI-D-15-0609.1.
Mochizuki, T., Kimoto, M., Watanabe, M., Chikamoto, Y., Ishii, M., 2016. Interbasin effects of the Indian Ocean on Pacific decadal climate change. Geophys. Res. Lett. 43, 7168–7175. https://doi.org/10.1002/2016GL069940.
Molteni, F., Farneti, R., Kucharski, F., Stockdale, T.N., 2017. Modulation of air-sea fluxes by extratropical planetary waves and its impact during the recent surface warming slowdown. Geophys. Res. Lett. 44, 1494–1502. https://doi.org/10.1002/2016GL072298.
Mori, M., Watanabe, M., Shiogama, H., Inoue, J., Kimoto, M., 2014. Robust Arctic Sea-ice influence on the frequent Eurasian cold winters in past decades. Nat. Geosci. 7, 869–873. https://doi.org/10.1038/ngeo2277.
Morice, C.P., Kennedy, J.J., Rayner, N.A., Jones, P.D., 2012. Quantifying uncertainties in global and regional temperature change using an ensemble of observational estimates: the HadCRUT4 data set. J. Geophys. Res. Atmos. 117. https://doi.org/10.1029/2011JD017187.
Newman, M., Alexander, M.A., Ault, T.R., Cobb, K.M., Deser, C., Di Lorenzo, E., Mantua, N.J., Miller, A.J., Minobe, S., Nakamura, H., Schneider, N., Vimont, D.J., Phillips, A.S., Scott, J.D., Smith, C.A., 2016. The Pacific decadal oscillation, revisited. J. Clim. 29, 4399–4427. https://doi.org/10.1175/JCLI-D-15-0508.1.
Nicolas, J.P., Bromwich, D.H., 2014. New reconstruction of Antarctic near-surface temperatures: Multidecadal trends and reliability of global reanalyses. J. Clim. 27, 8070–8093. https://doi.org/10.1175/JCLI-D-13-00733.1.
Nitta, T., Yamada, S., 1989. Recent warming of tropical sea surface temperature and its relationship to the Northern Hemisphere circulation. J. Meteorol. Soc. Japan 67, 375–383. https://doi.org/10.2151/jmsj1965.67.3_375.
Notz, D., Stroeve, J., 2016. Observed Arctic Sea-ice loss directly follows anthropogenic CO2 emission. Science 354, 747–750. https://doi.org/10.1126/science.aag2345.
Ogawa, F., Keenlyside, N., Gao, Y., Koenigk, T., Yang, S., Suo, L., Wang, T., Gastineau, G., Nakamura, T., Cheung, H.N., Omrani, N.E., Ukita, J., Semenov, V., 2018. Evaluating Impacts of recent Arctic Sea Ice loss on the Northern Hemisphere Winter Climate Change. Geophys. Res. Lett. 45, 3255–3263. https://doi.org/10.1002/2017GL076502.
Okumura, Y.M., 2013. Origins of tropical pacific decadal variability: Role of stochastic atmospheric forcing from the South Pacific. J. Clim. 26, 9791–9796. https://doi.org/10.1175/JCLI-D-13-00448.1.
Olonscheck, D., Mauritsen, T., Notz, D., 2019. Arctic sea-ice variability is primarily driven by atmospheric temperature fluctuations. Nat. Geosci. 12, 430–434 10.1038/s41561-019-0363-1.
Oudar, T., Kushner, P.J., Fyfe, J.C., Sigmond, M., 2018. No impact of anthropogenic aerosols on early 21st century global temperature trends in a large initial-condition ensemble. Geophys. Res. Lett. 45, 9245–9252. https://doi.org/10.1029/2018GL078841.
Overland, J.E., Wood, K.R., Wang, M., 2011. Warm Arctic-cold continents: climate impacts of the newly open arctic sea. Polar Res. 30. https://doi.org/10.3402/polar.v30i0.15787.
Overpeck, J., et al., 1997. Arctic environmental change of the last four centuries. Science 278, 1251–1256. https://doi.org/10.1126/science.278.5341.1251.
Palmer, M.D., McNeall, D.J., 2014. Internal variability of Earth's energy budget simulated by CMIP5 climate models. Environ. Res. Lett. 9https://doi.org/10.1088/1748-9326/9/3/034016. 034016.
Pan, Y.H., Oort, A.H., 1983. Global climate variations connected with sea surface temperature anomalies in the eastern equatorial Pacific Ocean for the 1958-73 period. Mon. Weather Rev. 111, 1244–1258. https://doi.org/10.1175/1520-0493(1983)111<1244:GCVCWS>2.0.CO;2.
Park, T., Park, W., Latif, M., 2016. Correcting North Atlantic Sea surface salinity biases in the Kiel climate Model: influences on ocean circulation and Atlantic Multidecadal Variability. Clim. Dyn. 47, 2543–2560. https://doi.org/10.1007/s00382-016-2982-1.
Petoukhov, V., Semenov, V.A., 2010. A link between reduced Barents-Kara Sea ice and cold winter extremes over northern continents. J. Geophys. Res. Atmos. 115https://doi.org/10.1029/2009JD013568. D21111.
Polvani, L.M., Waugh, D.W., Correa, G.J.P., Son, S.-W., 2011. Stratospheric ozone depletion: the main driver of twentieth-century atmospheric circulation changes in the Southern Hemisphere. J. Clim. 24, 795–812. https://doi.org/10.1175/2010JCLI3772.1.
Polyakov, I.V., et al., 2010. Arctic Ocean warming contributes to reduced polar ice cap. J. Phys. Oceanogr. 40, 2743–2756. https://doi.org/10.1175/2010JPO4339.1.
Polyakov, I.V., Pnyushkov, A.V., Alkire, M.B., Ashik, I.M., Baumann, T.M., Carmack, E.C., Goszczko, I., Guthrie, J., Ivanov, V.V., Kanzow, T., Krishfield, R., Kwok, R., Sundfjord, A., Morison, J., Rember, R., Yulin, A., 2017. Greater role for Atlantic inflows on sea-ice loss in the Eurasian Basin of the Arctic Ocean. Science 356, 285–291. https://doi.org/10.1126/science.aai8204.
Power, S., Casey, T., Folland, C., Colman, A., Mehta, V., 1999. Inter-decadal modulation of the impact of ENSO on Australia. Clim. Dyn. 15, 319–324. https://doi.org/10.1007/s003820050284.
Power, S., Delage, F., Chung, C., Kociuba, G., Keay, K., 2013. Robust twenty-first-century projections of El Niño and related precipitation variability. Nature 502, 541–545. https://doi.org/10.1038/nature12580.
Previdi, M., Liepert, B.G., 2007. Annular modes and Hadley cell expansion under global warming. Geophys. Res. Lett. 34https://doi.org/10.1029/2007GL031243. L22701.
Purich, A., England, M.H., Cai, W., Chikamoto, Y., Timmermann, A., Fyfe, J.C., Frankcombe, L., Meehl, G.A., Arblaster, J.M., 2016. Tropical Pacific SST drivers of recent Antarctic Sea ice trends. J. Clim. 29, 8931–8948. https://doi.org/10.1175/JCLI-D-16-0440.1.
Quan, X.W., Hoerling, M.P., Perlwitz, J., Diaz, H.F., 2018. On the time of emergence of tropical width change. J. Clim. 31, 7225–7236. https://doi.org/10.1175/JCLI-D-18-0068.1.
Robinson, W.A., 2002. On the midlatitude thermal response to tropical warmth. Geophys. Res. Lett. 29, 31. https://doi.org/10.1029/2001GL014158.
Ruprich-Robert, Y., Msadek, R., Castruccio, F., Yeager, S., Delworth, T., Danabasoglu, G., 2017. Assessing the climate impacts of the observed Atlantic multidecadal variability using the GFDL CM2.1 and NCAR CESM1 global coupled models. J. Clim. 30, 2785–2810. https://doi.org/10.1175/JCLI-D-16-0127.1.
Santer, B.D., Bonfils, C., Painter, J.F., Zelinka, M.D., Mears, C., Solomon, S., Schmidt,

G.A., Fyfe, J.C., Cole, J.N.S., Nazarenko, L., Taylor, K.E., Wentz, F.J., 2014. Volcanic contribution to decadal changes in tropospheric temperature. Nat. Geosci. 7, 185–189. https://doi.org/10.1038/ngeo2098.
Schmidt, D.F., Grise, K.M., 2017. The Response of Local Precipitation and Sea Level pressure to Hadley Cell expansion. Geophys. Res. Lett. 44, 10,573–10,582. https://doi.org/10.1002/2017GL075380.
Schmidt, G.A., Shindell, D.T., Tsigaridis, K., 2014. Reconciling warming trends. Nat. Geosci. 7, 158–160. https://doi.org/10.1038/ngeo2105.
Schneider, D.P., Steig, E.J., 2008. Ice cores record significant 1940s Antarctic warmth related to tropical climate variability. Proc. Natl. Acad. Sci. 105, 12154–12158. https://doi.org/10.1073/pnas.0803627105.
Screen, J.A., Deser, C., 2019. Pacific Ocean variability influences the time of emergence of a seasonally ice-free Arctic Ocean. Geophys. Res. Lett. 46, 2222–2231. https://doi.org/10.1029/2018GL081393.
Screen, J.A., Francis, J.A., 2016. Contribution of sea-ice loss to Arctic amplification is regulated by Pacific Ocean decadal variability. Nat. Clim. Chang. 6, 856–860. https://doi.org/10.1038/nclimate3011.
Screen, J.A., Simmonds, I., 2010a. The central role of diminishing sea ice in recent Arctic temperature amplification. Nature 464, 1334–1337. https://doi.org/10.1038/nature09051.
Screen, J.A., Simmonds, I., 2010b. Increasing fall-winter energy loss from the Arctic Ocean and its role in Arctic temperature amplification. Geophys. Res. Lett. 37https://doi.org/10.1029/2010GL044136. L16707.
Screen, J.A., Deser, C., Smith, D.M., Zhang, X., Blackport, R., Kushner, P.J., Oudar, T., McCusker, K.E., Sun, L., 2018. Consistency and discrepancy in the atmospheric response to Arctic Sea-ice loss across climate models. Nat. Geosci. 11, 155–163. https://doi.org/10.1038/s41561-018-0059-y.
Semenov, V.A., Latif, M., 2012. The early twentieth century warming and winter Arctic Sea ice. Cryosphere 6, 1231–1237. https://doi.org/10.5194/tc-6-1231-2012.
Seneviratne, S.I., Donat, M.G., Mueller, B., Alexander, L.V., 2014. No pause in the increase of hot temperature extremes. Nat. Clim. Chang. 4, 161–163. https://doi.org/10.1038/nclimate2145.
Serreze, M.C., Barry, R.G., 2011. Processes and impacts of Arctic amplification: a research synthesis. Glob. Planet. Chang. 77, 85–96. https://doi.org/10.1016/j.gloplacha.2011.03.004.
Serreze, M.C., Barrett, A.P., Stroeve, J.C., Kindig, D.M., Holland, M.M., 2009. The emergence of surface-based Arctic amplification. Cryosphere 3, 11–19. https://doi.org/10.5194/tc-3-11-2009.
Shimada, K., Kamoshida, T., Itoh, M., Nishino, S., Carmack, E., McLaughlin, F.A., Zimmermann, S., Proshutinsky, A., 2006. Pacific Ocean inflow: Influence on catastrophic reduction of sea ice cover in the Arctic Ocean. Geophys. Res. Lett. 33, L08605. https://doi.org/10.1029/2005GL025624.
Shindell, D., Faluvegi, G., 2009. Climate response to regional radiative forcing during the twentieth century. Nat. Geosci. 2, 294–300. https://doi.org/10.1038/ngeo473.
Si, D., Hu, A., 2017. Internally generated and externally forced multidecadal oceanic modes and their influence on the summer rainfall over East Asia. J. Clim. 30, 8299–8316. https://doi.org/10.1175/JCLI-D-17-0065.1.
Sigmond, M., Fyfe, J.C., 2010. Has the ozone hole contributed to increased Antarctic Sea ice extent? Geophys. Res. Lett. 37https://doi.org/10.1029/2010GL044301. L18502.
Sillmann, J., Donat, M.G., Fyfe, J.C., Zwiers, F.W., 2014. Observed and simulated temperature extremes during the recent warming hiatus. Environ. Res. Lett. 9https://doi.org/10.1088/1748-9326/9/6/064023. 064023.
Smirnov, D., Vimont, D.J., 2012. Extratropical forcing of tropical Atlantic variability during boreal summer and fall. J. Clim. 25, 2056–2076. https://doi.org/10.1175/JCLI-D-11-00104.1.
Smith, K.L., Polvani, L.M., Marsh, D.R., 2012. Mitigation of 21st century Antarctic sea ice loss by stratospheric ozone recovery. Geophys. Res. Lett. 39, L20701. https://doi.org/10.1029/2012GL053325.
Smith, D.M., et al., 2016. Role of volcanic and anthropogenic aerosols in the recent global surface warming slowdown. Nat. Clim. Chang. 6, 936–940. https://doi.org/10.1038/nclimate3058.
Smith, J.A., et al., 2017. Sub-ice-shelf sediments record history of twentieth-century retreat of Pine Island Glacier. Nature 541, 77–80. https://doi.org/10.1038/nature20136.
Smoliak, B.V., Wallace, J.M., Stoelinga, M.T., Mitchell, T.P., 2010. Application of partial least squares regression to the diagnosis of year-to-year variations in Pacific Northwest snowpack and Atlantic hurricanes. Geophys. Res. Lett. 37https://doi.org/10.1029/2009GL041478. L03801.
Staten, P.W., Rutz, J.J., Reichler, T., Lu, J., 2012. Breaking down the tropospheric circulation response by forcing. Clim. Dyn. 39, 2361–2375. https://doi.org/10.1007/s00382-011-1267-y.
Staten, P.W., Lu, J., Grise, K.M., Davis, S.M., Birner, T., 2018. Re-examining tropical expansion. Nat. Clim. Chang. 8, 768–775. https://doi.org/10.1038/s41558-018-0246-2.
Staten, P.W., Grise, K.M., Davis, S.M., Karnauskas, K., Davis, N., 2019. Regional Widening of Tropical Overturning: Forced Change, Natural Variability, and recent Trends. J. Geophys. Res. Atmos. 124, 6104–6119. https://doi.org/10.1029/2018JD030100.
Stroeve, J.C., Serreze, M.C., Holland, M.M., Kay, J.E., Malanik, J., Barrett, A.P., 2012. The Arctic's rapidly shrinking sea ice cover: a research synthesis. Clim. Chang. 110, 1005–1027. https://doi.org/10.1007/s10584-011-0101-1.
Stuecker, M.F., Bitz, C.M., Armour, K.C., 2017. Conditions leading to the unprecedented low Antarctic Sea ice extent during the 2016 austral spring season. Geophys. Res. Lett. 44, 9008–9019. https://doi.org/10.1002/2017GL074691.
Su, J., Zhang, R., Wang, H., 2017. Consecutive record-breaking high temperatures marked the handover from hiatus to accelerated warming. Sci. Rep. 7, 43735. https://doi.org/10.1038/srep43735.
Sun, L., Perlwitz, J., Hoerling, M., 2016. What caused the recent "warm Arctic, Cold Continents" trend pattern in winter temperatures? Geophys. Res. Lett. 43, 5345–5352. https://doi.org/10.1002/2016GL069024.
Sutton, R.T., Hodson, D.L.R., 2005. Ocean science: Atlantic Ocean forcing of north American and European summer climate. Science 309, 115–118. https://doi.org/10.1126/science.1109496.
Sutton, R.T., McCarthy, G.D., Robson, J., Sinha, B., Archibald, A.T., Gray, L.J., 2018. Atlantic multidecadal variability and the U.K. acsis program. Bull. Am. Meteorol. Soc. 99, 415–425. https://doi.org/10.1175/BAMS-D-16-0266.1.
Svendsen, L., Keenlyside, N., Bethke, I., Gao, Y., Omrani, N.E., 2018. Pacific contribution to the early twentieth-century warming in the Arctic. Nat. Clim. Chang. 8, 793–797. https://doi.org/10.1038/s41558-018-0247-1.
Takahashi, C., Watanabe, M., 2016. Pacific trade winds accelerated by aerosol forcing over the past two decades. Nat. Clim. Chang. 6, 768–772. https://doi.org/10.1038/nclimate2996.
Tao, L., Hu, Y., Liu, J., 2016. Anthropogenic forcing on the Hadley circulation in CMIP5 simulations. Clim. Dyn. 46, 3337–3350. https://doi.org/10.1007/s00382-015-2772-1.
Tatebe, H., Imada, Y., Mori, M., Kimoto, M., Hasumi, H., 2013. Control of decadal and bidecadal climate variability in the tropical pacific by the off-equatorial South Pacific Ocean. J. Clim. 26, 6524–6534. https://doi.org/10.1175/JCLI-D-12-00137.1.
Thoma, M., Greatbach, R.J., Kadow, C., Gerdes, R., 2015. Decadal hindcasts initialized using observed surface wind stress: Evaluation and prediction out to 2024. Geophys. Res. Lett. 42, 6454–6461. https://doi.org/10.1002/2015GL064833.
Thompson, D.W.J., Solomon, S., 2002. Interpretation of recent Southern Hemisphere climate change. Science 296, 895–899. https://doi.org/10.1126/science.1069270.
Thompson, D.W.J., Wallace, J.M., 2000. Annular modes in the extratropical circulation. Part I: month-to-month variability. J. Clim. 13, 1000–1016. https://doi.org/10.1175/1520-0442(2000)013%3C1000:AMITEC%3E2.0.CO;2.
Ting, M., Kushnir, Y., Li, C., 2014. North Atlantic Multidecadal SST Oscillation: External forcing versus internal variability. J. Mar. Syst. 133, 27–38. https://doi.org/10.1016/j.jmarsys.2013.07.006.
Tokinaga, H., Xie, S.P., Mukougawa, H., 2017. Early 20th-century Arctic warming intensified by Pacific and Atlantic multidecadal variability. Proc. Natl. Acad. Sci. U. S. A. 114, 6227–6232. https://doi.org/10.1073/pnas.1615880114.
Trenberth, K.E., Fasullo, J.T., 2010. Tracking earth's energy. Science 328, 316–317. https://doi.org/10.1126/science.1187272.
Trenberth, K.E., Shea, D.J., 2006. Atlantic hurricanes and natural variability in 2005. Geophys. Res. Lett. 33https://doi.org/10.1029/2006GL026894. L12704.
Trenberth, K.E., Caron, J.M., Stepaniak, D.P., Worley, S., 2002. Evolution of El Niño-Southern Oscillation and global atmospheric surface temperatures. J. Geophys. Res. D Atmos. 107https://doi.org/10.1029/2000JD000298. AAC 5-1-AAC 5-17.
Trenberth, K.E., Fasullo, J.T., Balmaseda, M.A., 2014a. Earth's energy imbalance. J. Clim. 27, 3129–3144. https://doi.org/10.1175/JCLI-D-13-00294.1.
Trenberth, K.E., Fasullo, J.T., Branstator, G., Phillips, A.S., 2014b. Seasonal aspects of the recent pause in surface warming. Nat. Clim. Chang. 4, 911–916. https://doi.org/10.1038/nclimate2341.
Trenberth, K.E., Zhang, Y., Fasullo, J.T., Taguchi, S., 2015. Climate variability and relationships between top-of-atmosphere radiation and temperatures on Earth. J. Geophys. Res. 120, 3642–3659. https://doi.org/10.1002/2014JD022887.
Turner, J., Comiso, J.C., Marshall, G.H., Lachlan-Cope, T.A., Bracegirdle, T., Maksym, T., Meredith, M.P., Wang, Z., Orr, A., 2009. Non-annular atmospheric circulation change induced by stratospheric ozone depletion and its role in the recent increase of Antarctic Sea ice extent. Geophys. Res. Lett. 36https://doi.org/10.1029/2009GL037524. L08502.
Vaughan, D.G., Comiso, J.C., Allison, I., Carrasco, J., Kaser, G., Kwok, R., Mote, P., Murray, T., Paul, F., Ren, J., Rignot, E., Solomina, O., Steffen, K., Zhang, T, 2013. Observations: Cryosphere. In: Stocker, T.F., Qin, D., Plattner, G.-K., Tignor, M., Allen, S.K., Boschung, J. ... Midgley, P.M. (Eds.), Climate Change 2013: The Physical Science Basis. Contribution of Working Group I to the Fifth Assessment Report of the Intergovernmental Panel on Climate Change. Cambridge University Press, Cambridge, United Kingdom and New York, NY, USA.
Villarini, G., Vecchi, G.A., 2013. Projected increases in North Atlantic tropical cyclone intensity from CMIP5 models. J. Clim. 26, 3231–3240. https://doi.org/10.1175/JCLI-D-12-00441.1.
Von Schuckmann, K., Palmer, M.D., Trenberth, K.E., Cazenave, A., Chambers, D., Champollion, N., Hansen, J., Josey, S.A., Loeb, N., Mathieu, P.P., Meyssignac, B., Wild, M., 2016. An imperative to monitor Earth's energy imbalance. Nat. Clim. Chang. https://doi.org/10.1038/nclimate2876.
Walker, C.C., Schneider, T., 2006. Eddy Influences on Hadley Circulations: Simulations with an Idealized GCM. J. Atmos. Sci. 63, 3333–3350. https://doi.org/10.1175/jas3821.1.
Wallace, J.M., Gutzler, D.S., 1981. Teleconnections in the geopotential height field during the Northern Hemisphere winter. Mon. Weather Rev. 109, 784–812. https://doi.org/10.1175/1520-0493(1981)109<0784:TITGHF>2.0.CO;2.
Wallace, J.M., Fu, Q., Smoliak, B.V., Lin, P., Johanson, C.M., 2012. Simulated versus observed patterns of warming over the extratropical Northern Hemisphere continents during the cold season. Proc. Natl. Acad. Sci. 109, 14337–14342. https://doi.org/10.1073/pnas.1204875109.
Wang, C., Dong, S., Evan, A.T., Foltz, G.R., Lee, S.K., 2012a. Multidecadal covariability of North Atlantic Sea surface temperature, African dust, Sahel Rainfall, and Atlantic hurricanes. J. Clim. 25, 5404–5415. https://doi.org/10.1175/JCLI-D-11-00413.1.
Wang, T., Otterå, O.H., Gao, Y., Wang, H., 2012b. The response of North Pacific Decadal Variability to strong tropical volcanic eruptions. Clim. Dyn. 39, 2917–2936. https://doi.org/10.1007/s00382-012-1373-5.
Wang, C., Xie, S.-P., Kosaka, Y., Liu, Q., Zheng, X., 2017a. Global i nfluence of t ropical

Pacific v ariability with i mplications for g lobal w arming s lowdown. J. Clim. 30, 2679–2695. https://doi.org/10.1175/JCLI-D-15-0496.1.
Wang, X., Li, J., Sun, C., Liu, T., 2017b. NAO and its relationship with the Northern Hemisphere mean surface temperature in CMIP5 simulations. J. Geophys. Res. 122, 4202–4227. https://doi.org/10.1002/2016JD025979.
Watanabe, M., Shiogama, H., Tatebe, H., Hayashi, M., Ishii, M., Kimoto, M., 2014. Contribution of natural decadal variability to global warming acceleration and hiatus. Nat. Clim. Chang. 4, 893–897. https://doi.org/10.1038/nclimate2355.
Wegmann, M., Bronnimann, S., Compo, G.P., 2017. Tropospheric circulation during the early twentieth century Arctic warming. Clim. Dyn. 48, 2405–2418. https://doi.org/10.1007/s00382-016-3212-6.
Wittman, M.A.H., Charlton, A.J., Polvani, L.M., 2007. The effect of lower Stratospheric Shear on Baroclinic Instability. J. Atmos. Sci. 64, 479–496. https://doi.org/10.1175/jas3828.1.
Wood, K.R., Overland, J.E., 2010. Early 20th century Arctic warming in retrospect. Int. J. Climatol. 30, 1269–1279. https://doi.org/10.1002/joc.1973.
Woodgate, R.A., Aagaard, K., Weingartner, T.J., 2006. Interannual changes in the Bering Strait fluxes of volume, heat and freshwater between 1991 and 2004. Geophys. Res. Lett. 33, L156. https://doi.org/10.1029/2006GL026931.
Wu, T., Hu, Z., Gao, F., Zhang, J., Meehl, G.A., 2019. New insights into natural variability and anthropogenic forcing of global/regional climate evolution. npj Clim. Atmos. Sci. 2, 18. https://doi.org/10.1038/s41612-019-0075-7.
Xie, S.-P., 2020. Ocean warming pattern effect on global and regional climate change. AGU Adv. 1https://doi.org/10.1029/2019AV000130. accepted.
Xie, S.-P., Kosaka, Y., 2017. What Caused the Global Surface Warming Hiatus of 1998-2013? Curr. Clim. Chang. Reports 3, 128–140. https://doi.org/10.1007/s40641-017-0063-0.
Xie, S.P., Deser, C., Vecchi, G.A., Ma, J., Teng, H., Wittenberg, A.T., 2010. Global warming pattern formation: Sea surface temperature and rainfall. J. Clim. 23, 966–986. https://doi.org/10.1175/2009JCLI3329.1.
Xie, S.P., Kosaka, Y., Okumura, Y.M., 2016. Distinct energy budgets for anthropogenic and natural changes during global warming hiatus. Nat. Geosci. 9, 29–33. https://doi.org/10.1038/ngeo2581.
Xu, Y., Hu, A., 2018. How would the twenty-first-century warming influence Pacific decadal variability and its connection to north American rainfall: Assessment based on a revised procedure for the IPO/PDO. J. Clim. 31, 1547–1563. https://doi.org/10.1175/JCLI-D-17-0319.1.
Yamanouchi, T., 2011. Early 20th century warming in the Arctic: a review. Polar Sci. 5, 53–71. https://doi.org/10.1016/j.polar.2010.10.002.
Yan, X., Zhang, R., Knutson, T.R., 2017. The role of Atlantic overturning circulation in the recent decline of Atlantic major hurricane frequency. Nat. Commun. 8, 1695. https://doi.org/10.1038/s41467-017-01377-8.
Yan, X., Zhang, R., Knutson, T.R., 2018. Underestimated AMOC Variability and Implications for AMV and Predictability in CMIP Models. Geophys. Res. Lett. 45, 4319–4328. https://doi.org/10.1029/2018GL077378.
Yang, X.-Y., Fyfe, J.C., Flato, G.M., 2010. The role of poleward energy transport in Arctic temperature evolution. Geophys. Res. Lett. 37https://doi.org/10.1029/2010GL043934. L14803.
Ye, J.S., 2014. Trend and variability of China's summer precipitation during 1955-2008. Int. J. Climatol. 34, 559–566. https://doi.org/10.1002/joc.3705.
Yuan, T., Oreopoulos, L., Zelinka, M., Yu, H., Norris, J.R., Chin, M., Platnick, S., Meyer, K., 2016. Positive low cloud and dust feedbacks amplify tropical North Atlantic Multidecadal Oscillation. Geophys. Res. Lett. 43, 1349–1356. https://doi.org/10.1002/2016GL067679.
Zhang, R., 2015. Mechanisms for low-frequency variability of summer Arctic Sea ice extent. Proc. Natl. Acad. Sci. 112, 4570–4575. https://doi.org/10.1073/pnas.1422296112.
Zhang, R., 2017. On the persistence and coherence of subpolar sea surface temperature and salinity anomalies associated with the Atlantic multidecadal variability. Geophys. Res. Lett. 44, 7865–7875. https://doi.org/10.1002/2017GL074342.
Zhang, R., Delworth, T.L., 2006. Impact of Atlantic multidecadal oscillations on India/Sahel rainfall and Atlantic hurricanes. Geophys. Res. Lett. 33https://doi.org/10.1029/2006GL026267. L17712.
Zhang, R., Delworth, T.L., 2007. Impact of the Atlantic Multidecadal Oscillation on North Pacific climate variability. Geophys. Res. Lett. 34https://doi.org/10.1029/2007GL031601. L23708.
Zhang, L., Delworth, T.L., 2015. Analysis of the characteristics and mechanisms of the pacific decadal oscillation in a suite of coupled models from the geophysical fluid dynamics laboratory. J. Clim. 28, 7678–7701. https://doi.org/10.1175/JCLI-D-14-00647.1.
Zhang, H., Delworth, T.L., 2018. Detectability of decadal anthropogenic hydroclimate changes over North Americ. J. Clim. 31, 2579–2597. https://doi.org/10.1175/JCLI-D-17-0366.1.
Zhang, Y., Wallace, J.M., Battisti, D.S., Zhang, Y., Wallace, J.M., Battisti, D.S., 1997. ENSO-like Interdecadal Variability: 1900–93. J. Clim. 10, 1004–1020. https://doi.org/10.1175/1520-0442(1997)010<1004:ELIV>2.0.CO;2.
Zhang, R., Delworth, T.L., Dixon, K.W., Held, I.M., Ming, Y., Msadek, R., Rosati, A.J., Vecchi, G.A., Sutton, R., Hodson, D.L.R., Robson, J., Kushnir, Y., Ting, M., Marshall, J., 2013a. Have aerosols caused the observed Atlantic multidecadal variability? J. Atmos. Sci. 70, 1135–1144. https://doi.org/10.1175/JAS-D-12-0331.1.
Zhang, X., He, J., Zhang, J., Polaykov, I., Gerdes, R., Inoue, J., Wu, P., 2013b. Enhanced poleward moisture transport and amplified northern high-latitude wetting trend. Nat. Clim. Chang. 3, 47–51. https://doi.org/10.1038/nclimate1631.
Zhang, R., Sutton, R., Danabasoglu, G., Delworth, T.L., Kim, W.M., Robson, J., Yeager, S.G., 2016. Comment on "The Atlantic Multidecadal Oscillation without a role for ocean circulation.". Science 352, 1527. https://doi.org/10.1126/science.aaf1660.
Zhang, P., Wu, Y., Simpson, I.R., Smith, K.L., Zhang, X., De, B., Callaghan, P., 2018a. A stratospheric pathway linking a colder Siberia to Barents-Kara Sea Sea ice loss. Sci. Adv. 4https://doi.org/10.1126/sciadv.aat6025. eaat6025.
Zhang, Y., Xie, S.P., Kosaka, Y., Yang, J.C., 2018b. Pacific decadal oscillation: Tropical Pacific forcing versus internal variability. J. Clim. 31, 8265–8279. https://doi.org/10.1175/JCLI-D-18-0164.1.
Zhang, H.-M., Lawrimore, J.H., Huang, B., Menne, M.J., Yin, X., Sánchez-Lugo, A., Gleason, B.E., Vose, R., Arndt, D., Rennie, J.J., Williams, C.N., 2019a. The NOAA Global Surface Temperature Dataset Version 5: Employing Improved Data Coverage and Historical Homogenization. AGU Eos. (in press).
Zhang, L., Delworth, T.L., Cooke, W., Yang, X., 2019b. Natural variability of Southern Ocean convection as a driver of observed climate trends. Nat. Clim. Chang. 9, 59–65. https://doi.org/10.1038/s41558-018-0350-3.
Zhang, R., Sutton, R., Danabasoglu, G., Kwon, Y.O., Marsh, R., Yeager, S.G., Amrhein, D.E., Little, C.M., 2019c. A Review of the role of the Atlantic Meridional Overturning Circulation in Atlantic Multidecadal Variability and associated climate impacts. Rev. Geophys. 57, 316–375. https://doi.org/10.1029/2019RG000644.
Zhou, C., Zelinka, M.D., Dessler, A.E., Klein, S.A., 2015. The relationship between interannual and long-term cloud feedbacks. Geophys. Res. Lett. 42, 10463–10469. https://doi.org/10.1002/2015GL066698.
Zhou, C., Zelinka, M.D., Klein, S.A., 2016. Impact of decadal cloud variations on the Earth's energy budget. Nat. Geosci. 9, 871–874. https://doi.org/10.1038/ngeo2828.
Zhou, C., Zelinka, M.D., Klein, S.A., 2017. Analyzing the dependence of global cloud feedback on the spatial pattern of sea surface temperature change with a Green's function approach. J. Adv. Model. Earth Syst. 9, 2174–2189. https://doi.org/10.1002/2017MS001096.